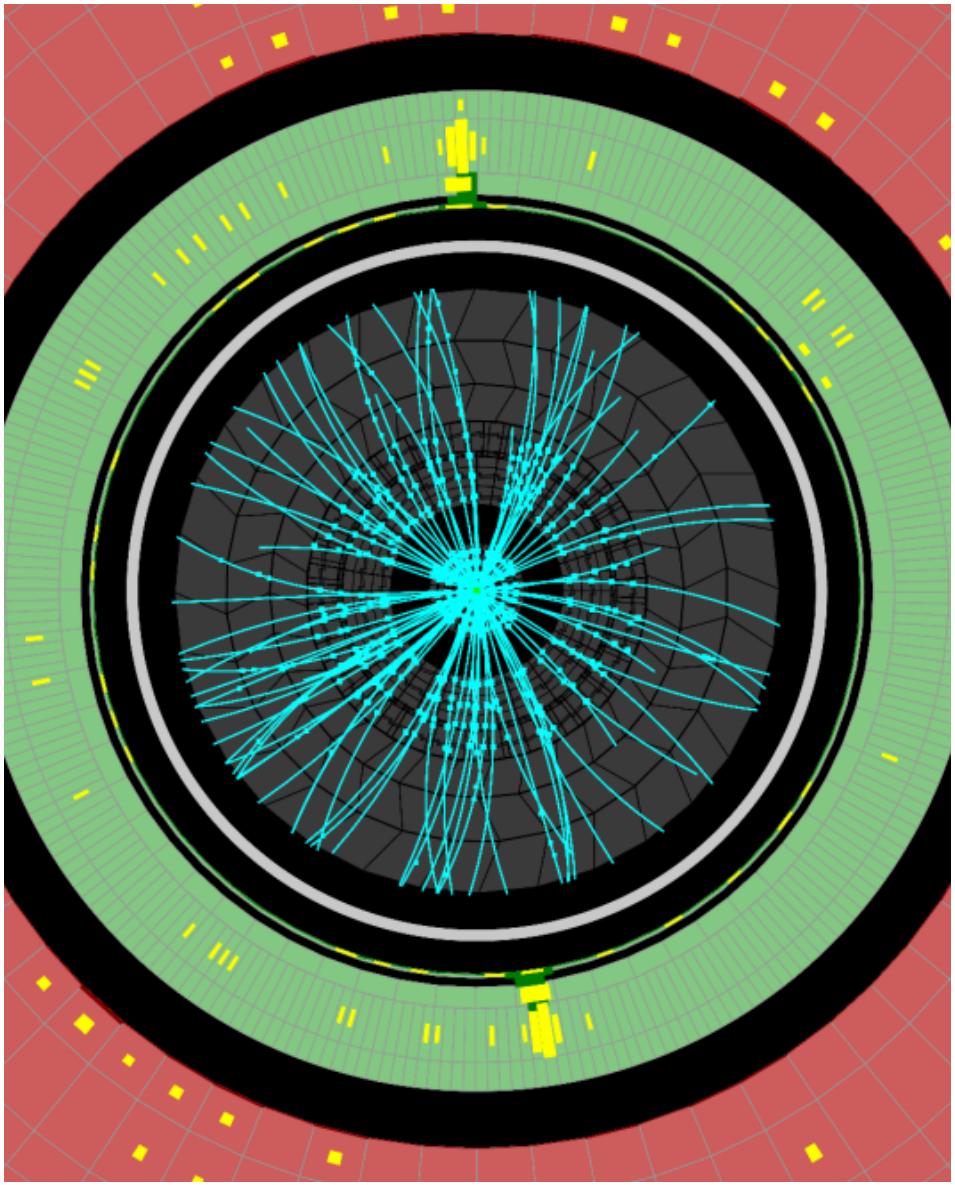

$H \to \gamma\gamma$ measurements at the ATLAS experiment

LBL Research Progress Meeting
Aug 12, 2014

Kerstin Tackmann

The Standard Model and the Higgs boson.

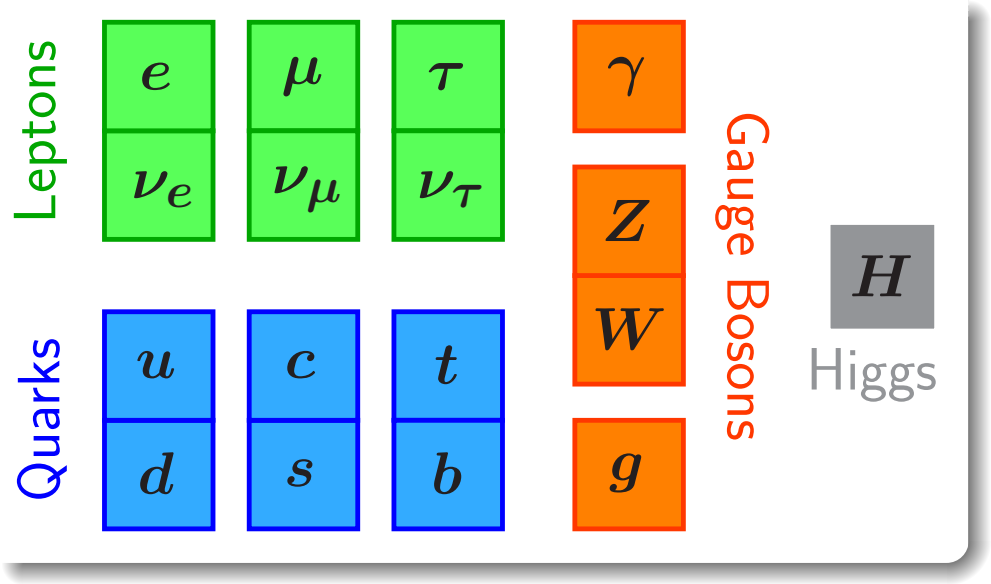

SM describes known elementary particles and their interactions

Local gauge invariance does not allow explicit mass terms in the Lagrangian – but experiment shows W and Z to have mass

- Elementary particles acquire mass through the Higgs (BEH) mechanism by interacting with the Higgs field
  - ⋆ Introduced 1964 by Brout, Englert and Higgs

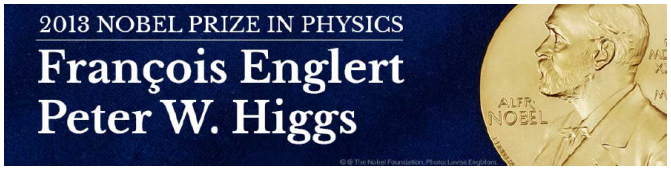

- Candidate discovered by the ATLAS and CMS experiments (2012)

What do we expect a SM Higgs boson to look like?

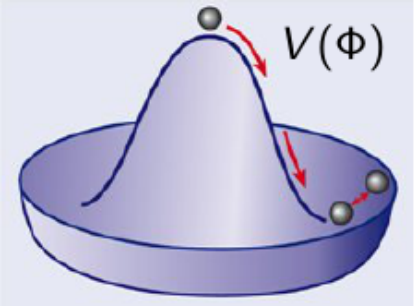

Introduce a scalar field with vaccum expectation value $v \neq 0$

$$\phi(x) = \begin{pmatrix} \phi^+(x) \\ \phi^0(x) \end{pmatrix} \rightarrow \langle \phi \rangle = \frac{1}{\sqrt{2}} \begin{pmatrix} 0 \\ v \end{pmatrix} \text{ (unitary gauge)}$$

Mass terms from interaction between Higgs field and gauge bosons and fermions:

$$\mathcal{L}_\phi = (D^\mu \phi)^\dagger (D_\mu \phi) - g_f(\bar{\psi}_L \phi \psi_R + \bar{\psi}_R \phi \psi_L) - V(\phi)$$

- Gauge boson masses $m_{W^\pm} = \frac{gv}{2}$, $m_Z = \frac{v\sqrt{g^2 + g'^2}}{2}$
- Charged fermion masses $m_f = \frac{g_f v}{\sqrt{2}}$
  - ⋆ Not needed for electroweak symmetry breaking, but convenient to generate fermion masses

Higgs mechanism predicts the existence of a new, neutral boson: the Higgs boson, coupling to particles proportional to their mass, $J^P = 0^+$

The Large Hadron Collider and the ATLAS experiment.

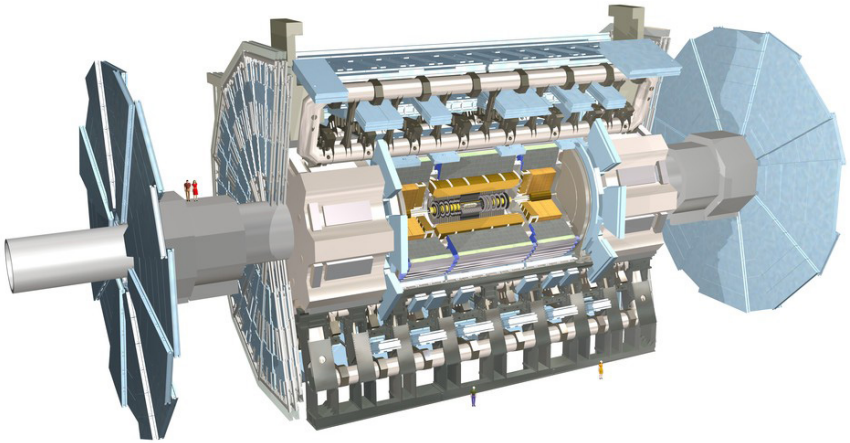

LHC

- Proton-proton collisions
  - ⋆ 2010/11 $\sqrt{s} = 7$ TeV (6 fb^{-1})
  - ⋆ 2012 $\sqrt{s} = 8$ TeV (23 fb^{-1})
- 2013/14 shutdown: machine and detector consolidation+upgrade
- 2015- pp collisions at 13-14 TeV

ATLAS

- Multipurpose detector: search for new physics, Higgs, top and SM measurements, ...

Outstanding performance of LHC and the experiments

The cost of high luminosity: pileup.

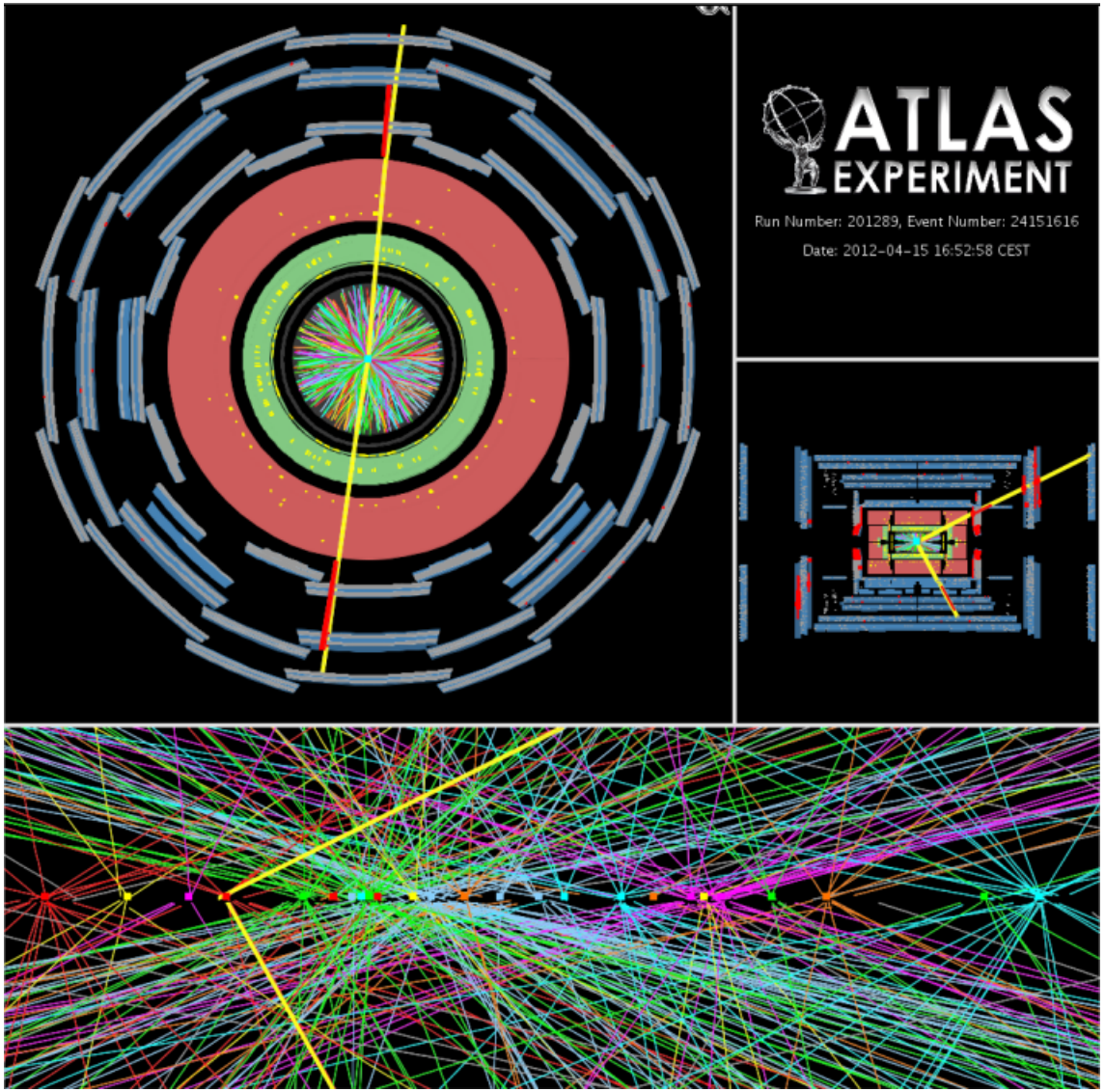

$Z \to \mu\mu$ with 25 interaction vertices

[ATLAS public plots]

Challenge to trigger, software and analyses

- → Large amount of data to process and store
- → Identification and measurement of the "interesting" objects, including the primary vertex

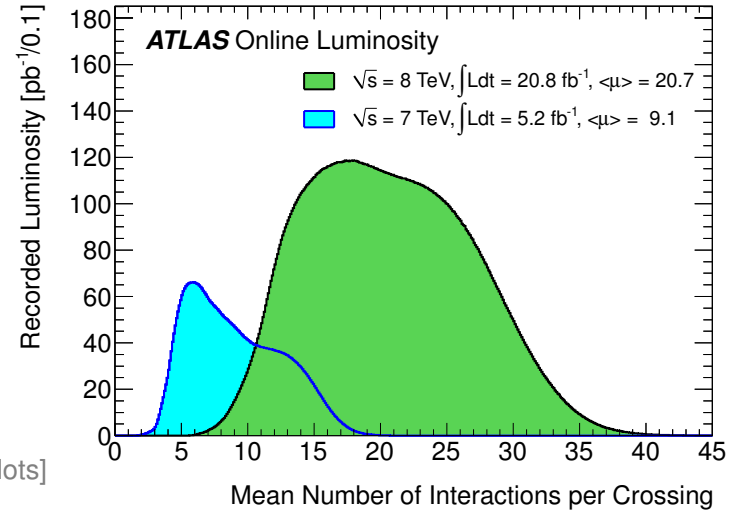

Higgs boson production at the LHC.

Gluon fusion: 19.5 pb

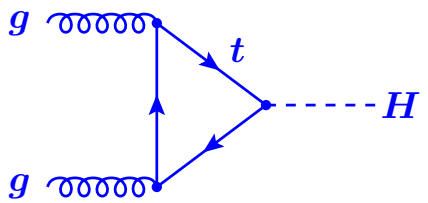

Higgs tends to have low p_T

Associated production: 1.1 pb

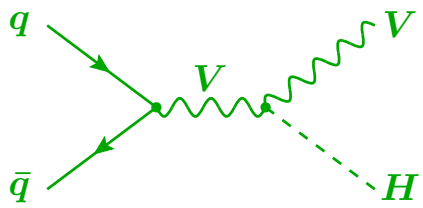

Clear signature: reconstruct W and Z in leptonic and/or hadronic decays

Vector boson fusion: 1.6 pb

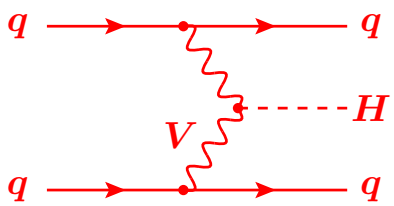

Distinct signature with 2 forward jets and little hadronic activity in between

Associated production with $t\bar{t}$: 0.1 pb

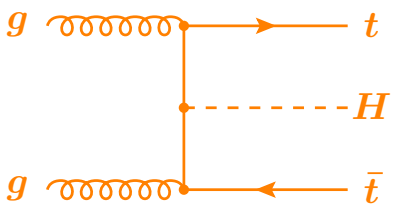

Tag presence of two top quarks

Production cross sections given at m_H =125 GeV and $\sqrt{s}$ =8 TeV

SM Higgs boson decays.

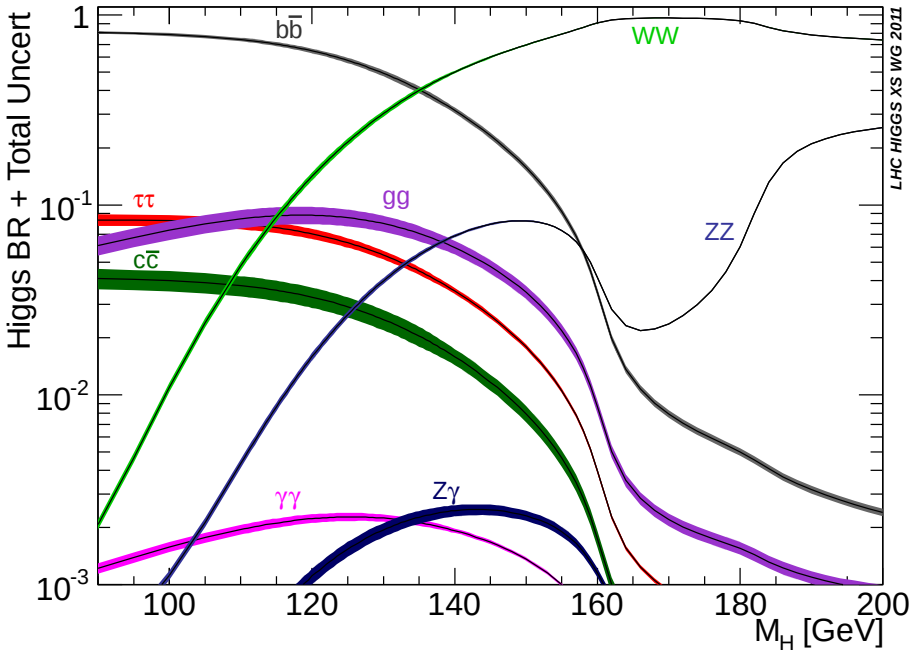

Higgs boson couples to mass

Decay branching fractions @ $m_H =$ 125 GeV

$H \to b\bar{b}$	57.7%
$H \to WW$	21.5%
$H \to \tau\tau$	6.3%
$H \to ZZ$	2.6%
$H \to \gamma\gamma$	0.23%

$H \to \gamma\gamma$: Comparably simple final state: 2 energetic isolated photons

Large event yield despite low branching fractions expect to see 475 signal events in current dataset

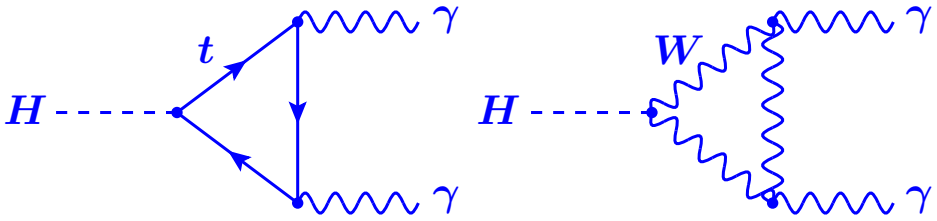

Decay through loop processes → sensitive to new heavy particles

What do we need for $H \to \gamma\gamma$?

efficient γ reconstruction + good separation of converted and unconverted γ

efficient γ identification, large rejection of hadronic background

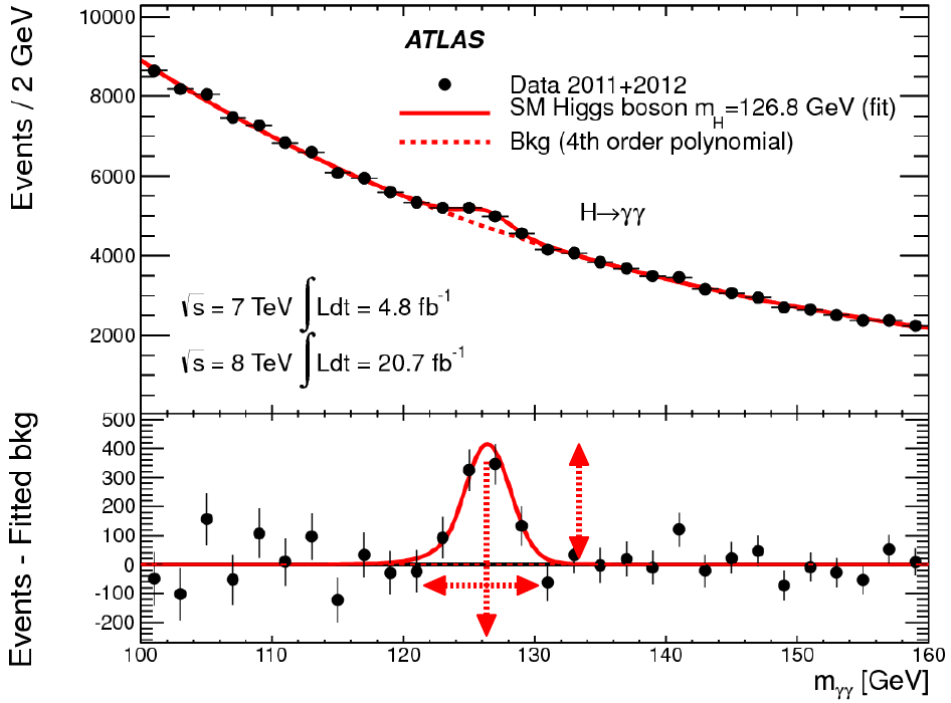

precise calibration of γ energy scale, good resolution

performant $\gamma\gamma$ trigger, compromise between high signal acceptance and low enough rate

Photon reconstruction, identification and calibration

ATLAS Inner Detector (ID) and EM Calorimeter.

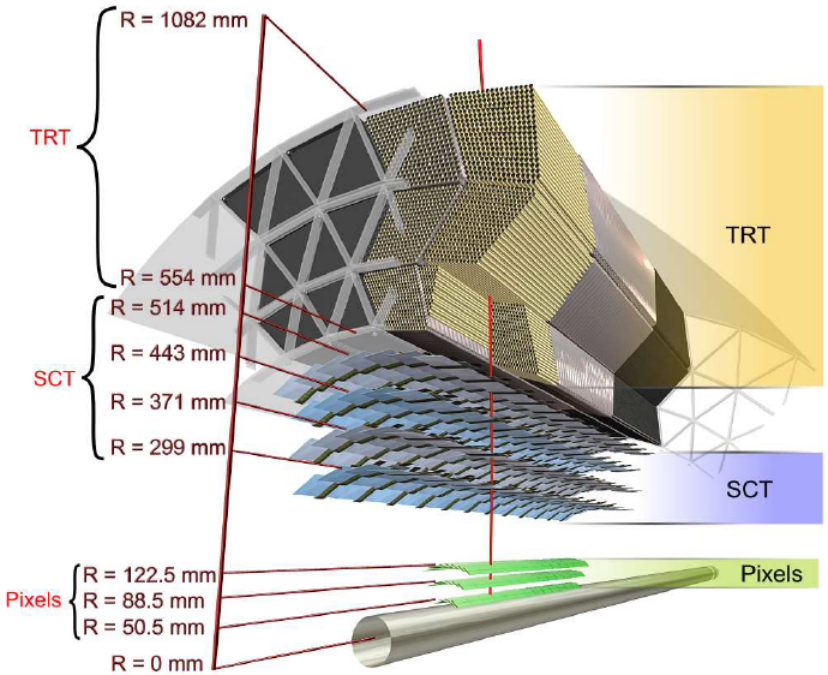

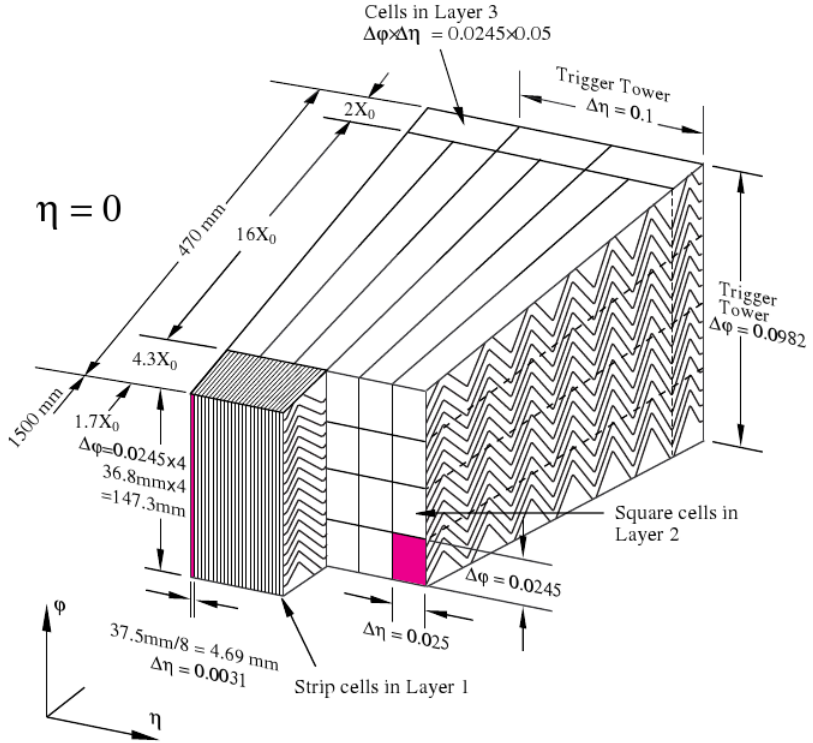

$|\eta| < 2.5$, barrel-endcaps geometry

- 3 layers Si Pixel
- 4 double layers Si strips (SCT)
- straw-tube Transition Radiation Tracker (TRT)
  - ⋆ $e^{\pm}$ identification capabilities through transition radiation

$|\eta| < 3.2$, barrel-endcaps geometry

- Pb-LAr sampling calorimeter
- 3 longitudinal layers with accordion geometry and presampler inside of cryostat
- Fine granularity allows measurement of shower shape

Photon reconstruction.

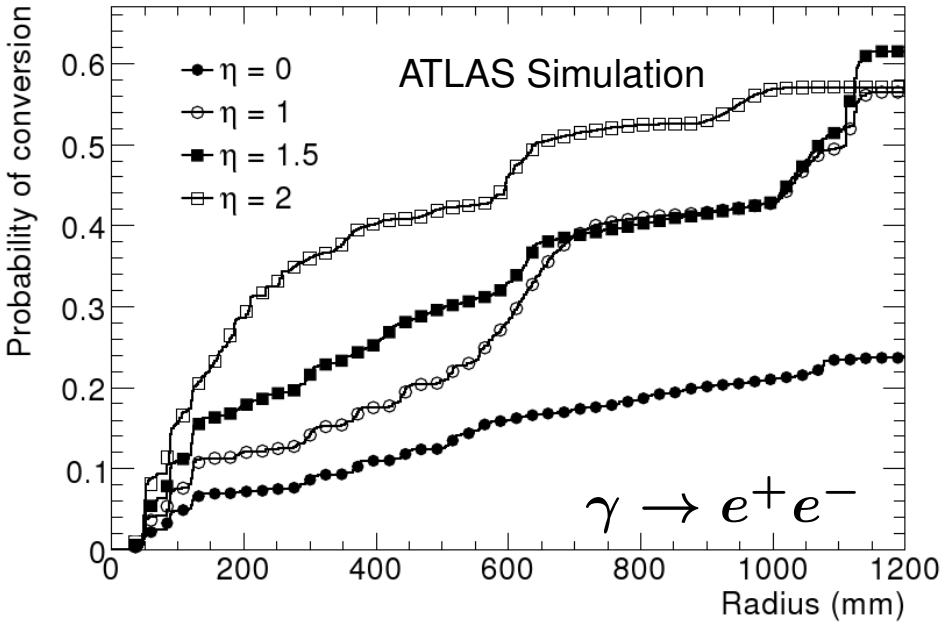

- ∼ 40% of photons convert before reaching the calorimeter
- Efficient reconstruction of converted photons needed for dedicated
  - ⋆ photon energy calibration
  - ⋆ photon identification

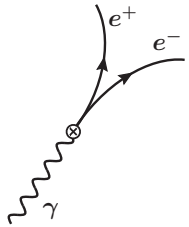

[ATLAS-CONF-2011-128]

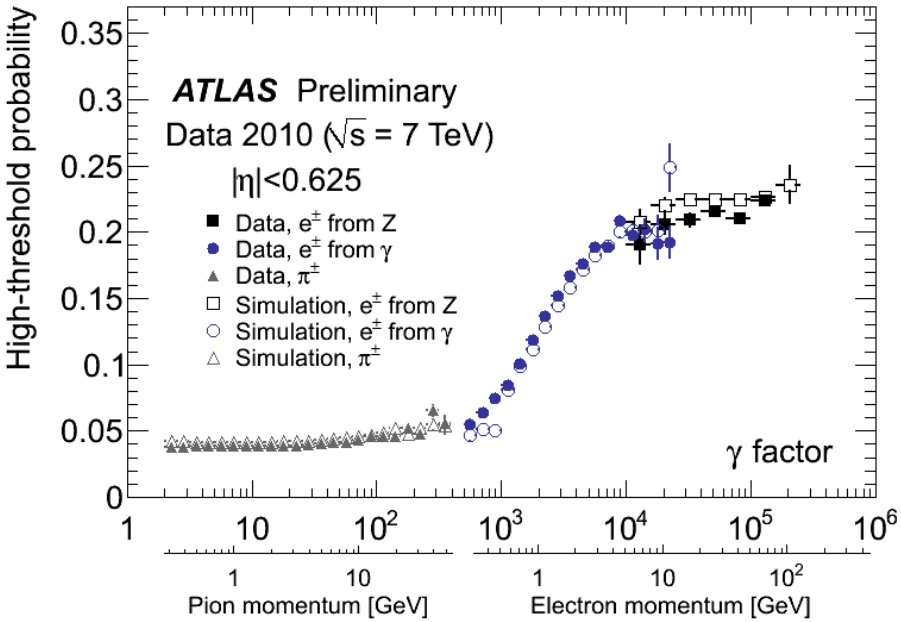

- Conversion tracks from
  - ⋆ Inside-out tracking seeded in Si detectors
  - ⋆ Back-tracking seeded in TRT and extended into Si
  - ⋆ Standalone TRT tracking
- Track selection relies on transition radiation in TRT

Photon reconstruction (8 TeV).

[ATLAS-CONF-2011-161]

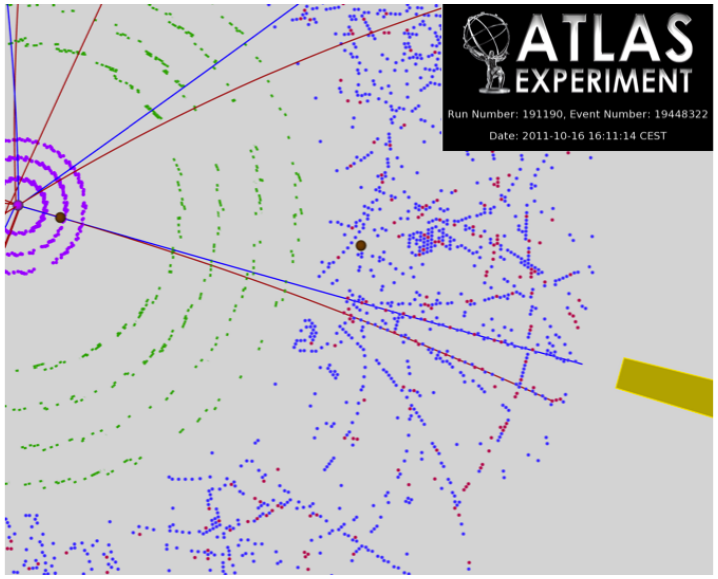

- Reconstruction of conversion vertices seeded from loosely selected electromagnetic clusters
  - ⋆ 2-track vertices consistent with decay of massless particle
  - ⋆ “1-track vertices” missing hits in innermost layer(s)
- Reconstructed secondary vertices (and tracks) matched to clusters in calorimeter
- Clusters without matching vertices or tracks: unconverted photons
- Reconstruction robust against pileup

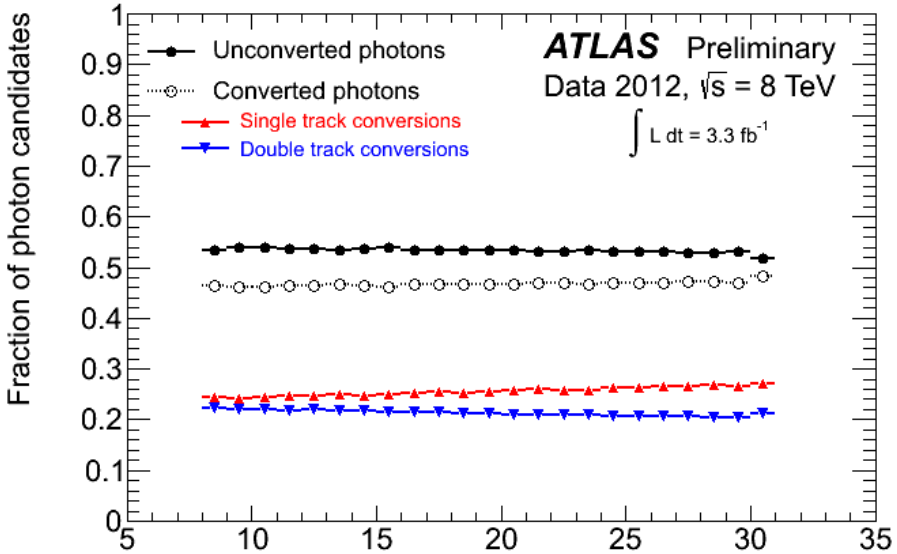

[ATLAS public plot] Average interactions per bunch crossing

Photon identification.

- Powerful jet-rejection ($\mathcal{O}(10^4)$) needed to suppress dominant hadronic background
- Fine granularity of electromagnetic calorimeter allows photon identification based on shower shape

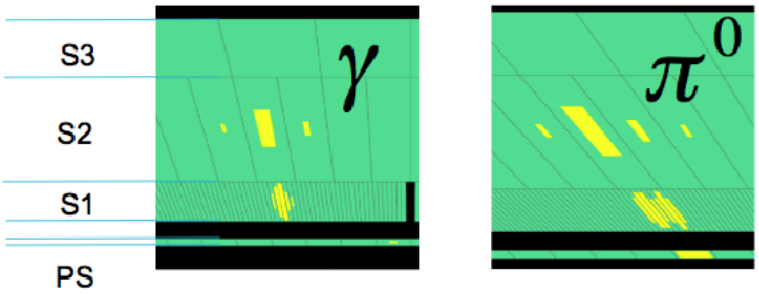

[ATLAS public figure]

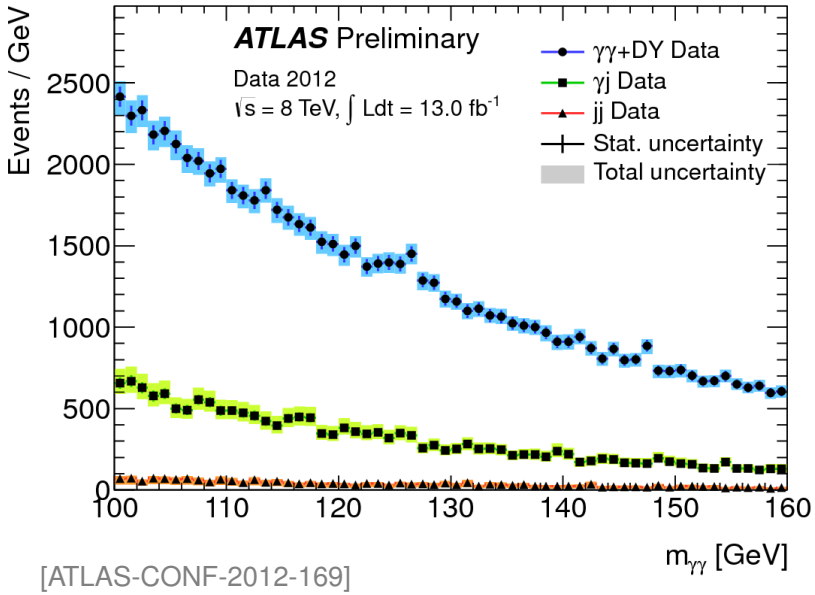

[ATLAS-CONF-2012-169]

After photon identification and requiring photon candidates to be isolated in calorimeter and tracker

75% $\gamma\gamma$ events
22% γ-jet events
3% jet-jet events

Efficiency measurements.

[ATLAS-CONF-2012-123]

Id efficiency for isolated photons: E_T^{iso} <4 GeV

Radiative Z decays: $Z \to \ell\ell\gamma$

E_T^{γ} of 10-80 GeV

Photon purity

- $\sim$ 90% (10-15 GeV)
- $\geq$ 98% ($>$ 15 GeV)

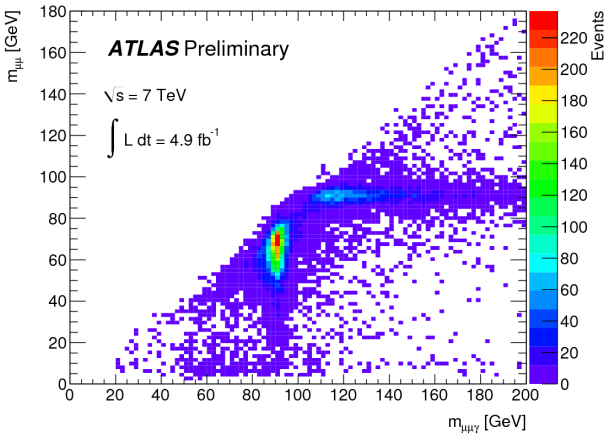

$Z \to ee$ tag-and-probe

+ transformation of electron showers to resemble photon showers

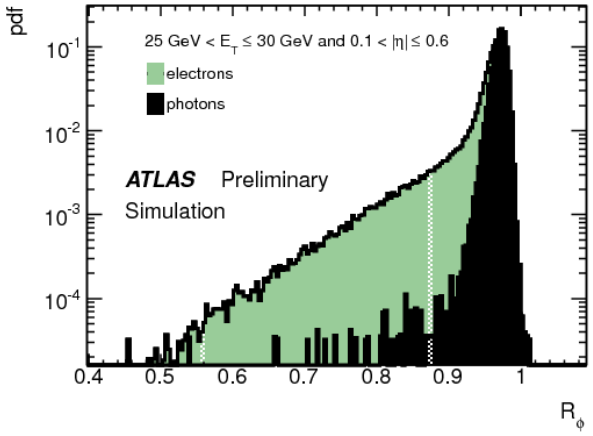

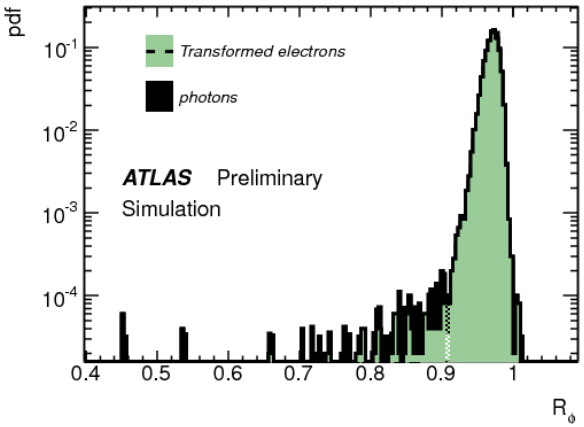

"Matrix method"

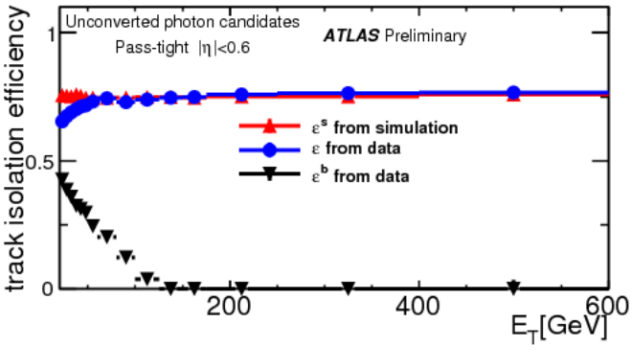

Purity determination from track isolation before and after id $\to$ id efficiency

Efficiency measurements.

[ATLAS public plots]

- Partial overlap in E_T regions covered by the different methods

→ Combination of measurements in overlap regions

- 1-2% uncertainties for $E_T <$ 40 GeV, 0.5-1% above 40 GeV

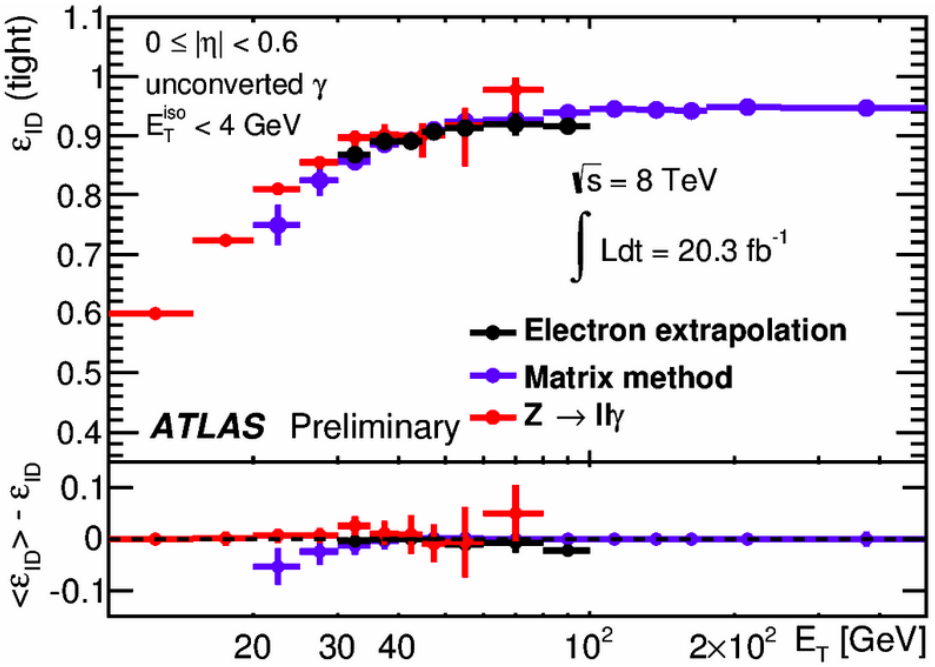

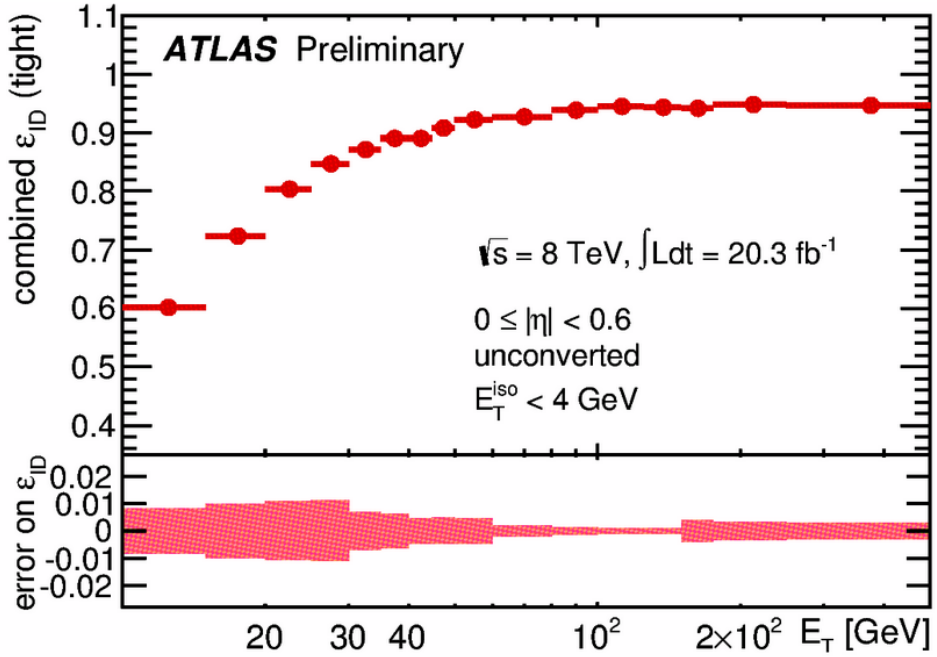

Uncertainty on $H \to \gamma\gamma$ signal yield

ICHEP 2012	10.8%
Dec 2012	5.3%
Moriond 2013	2.4%
ICHEP 2014	1%

Second-largest experimental uncertainty on $H \to \gamma\gamma$ signal strength (Phys. Lett. B 726 (2013))

Energy calibration.

Electron and photon energy calibration completely revisited

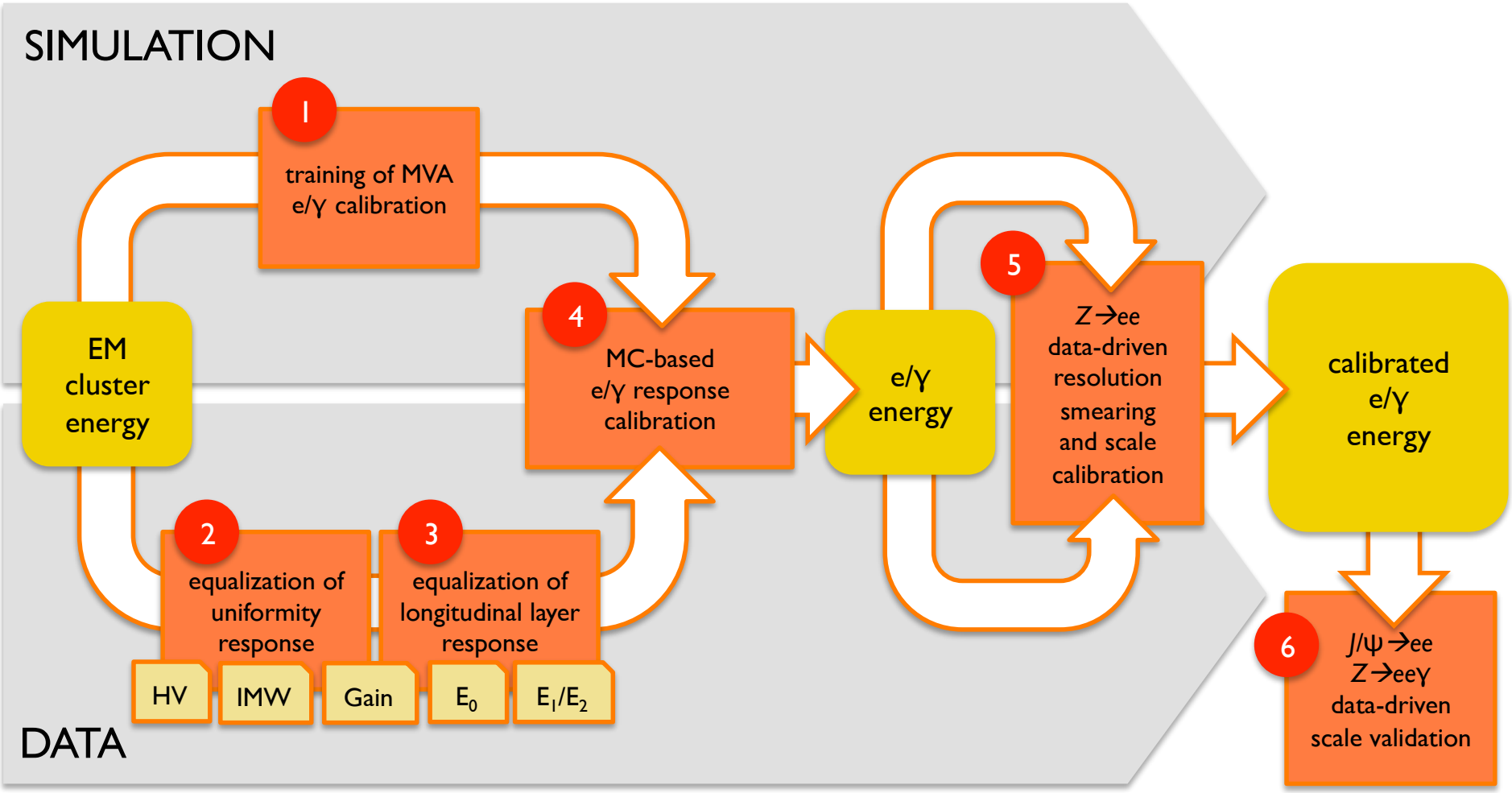

Energy calibration.

- Longitudinal shower shapes of μ, e and unconverted γ used to determine material upstream of calorimeter and relative calibration of calorimeter layers
- Improved simulation of upstream material
  - ★ Radiation length can be measured to 4-6% X_0

[arXiv:1407.5063]

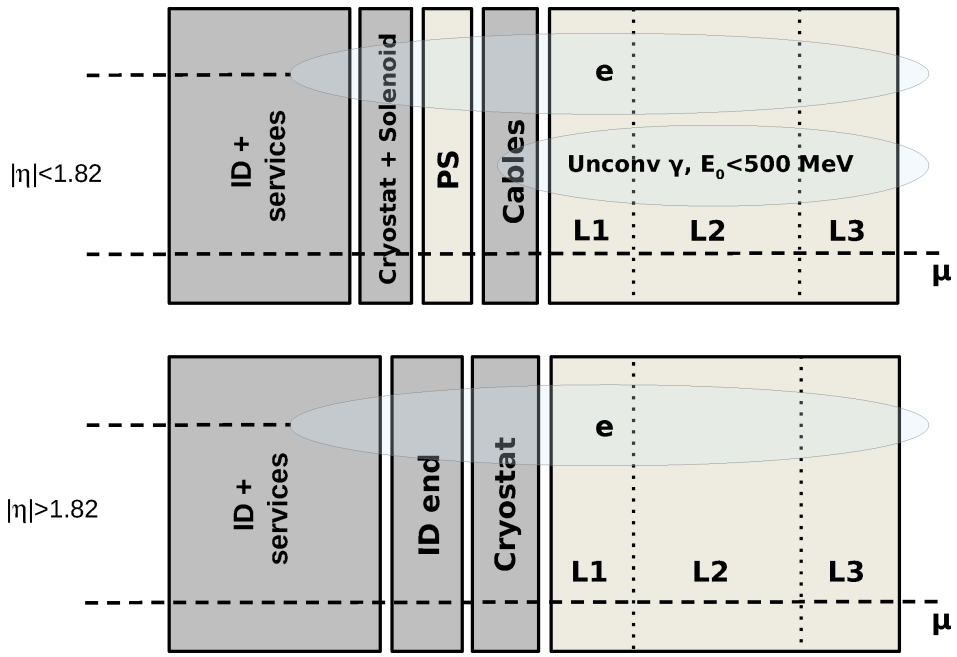

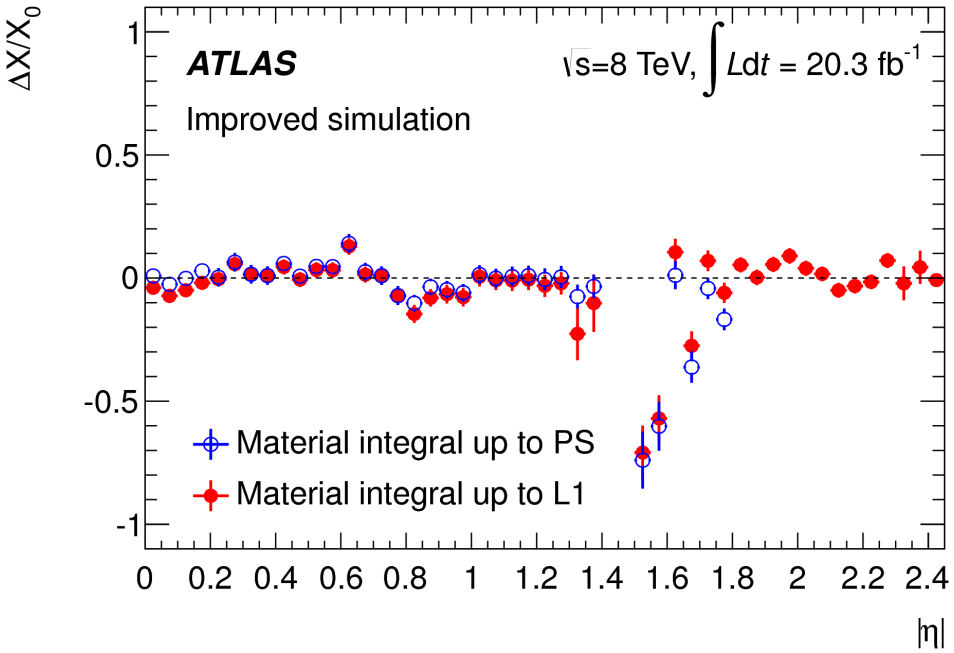

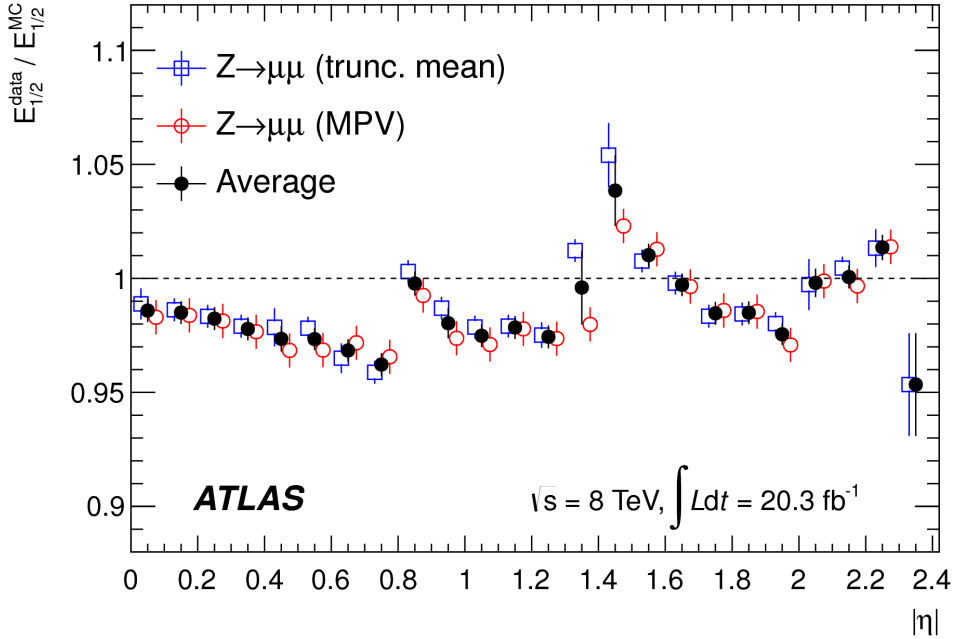

Energy calibration.

- New MC-based energy calibration (separate for e, converted and unconverted γ)
  - ⋆ Improvement of $\gamma\gamma$ invariant mass resolution of $\sim$10%
- Absolute energy scale determined from $Z \to ee$
  - ⋆ Typical uncertainty $\mathbf{0.05\%}$ in most detector regions, up to $\mathbf{0.2\%}$ in regions with large amounts of passive material
- Energy scale stable with pileup within $\mathbf{0.05\%}$

[arXiv:1407.5063]

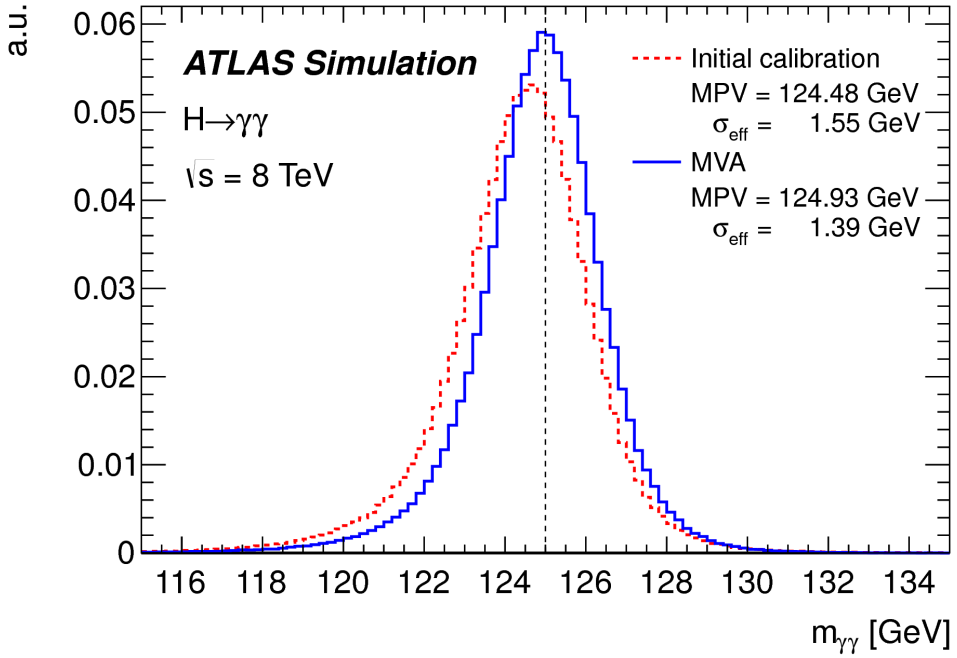

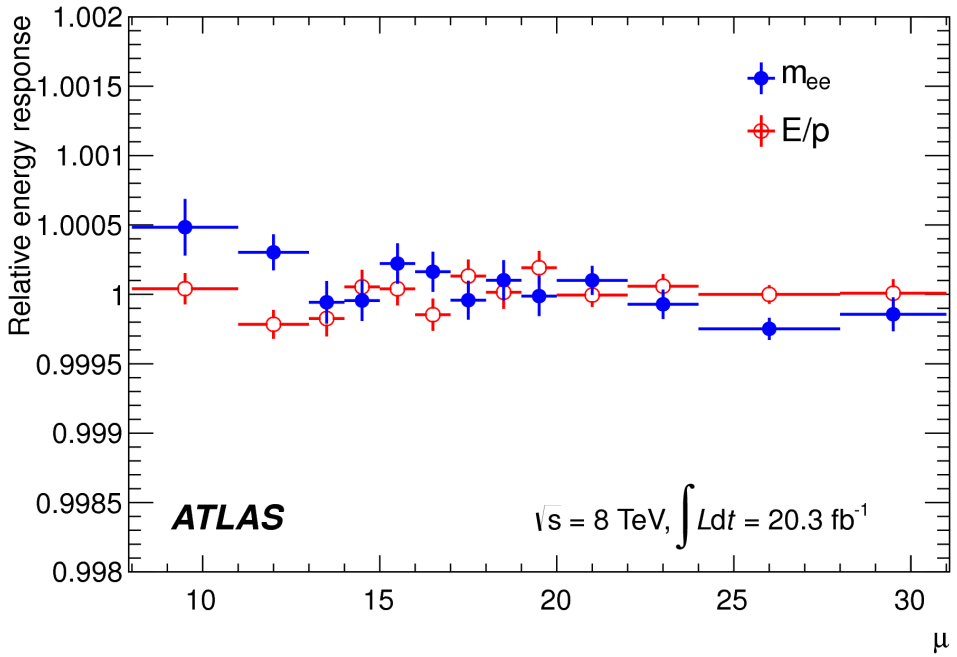

Energy calibration.

Cross checks

- Energy scale measured from $Z \to \ell\ell\gamma$ agrees within uncertainties
- Linearity checked with J/ψ and $Z \to ee$

Resolution

- Resolution correction obtained from $Z \to ee$
- Uncertainties
  - ⋆ $Z \to ee$ measurement
  - ⋆ Material simulation
  - ⋆ Calorimeter sampling term
  - ⋆ Pileup

[arXiv:1407.5063]

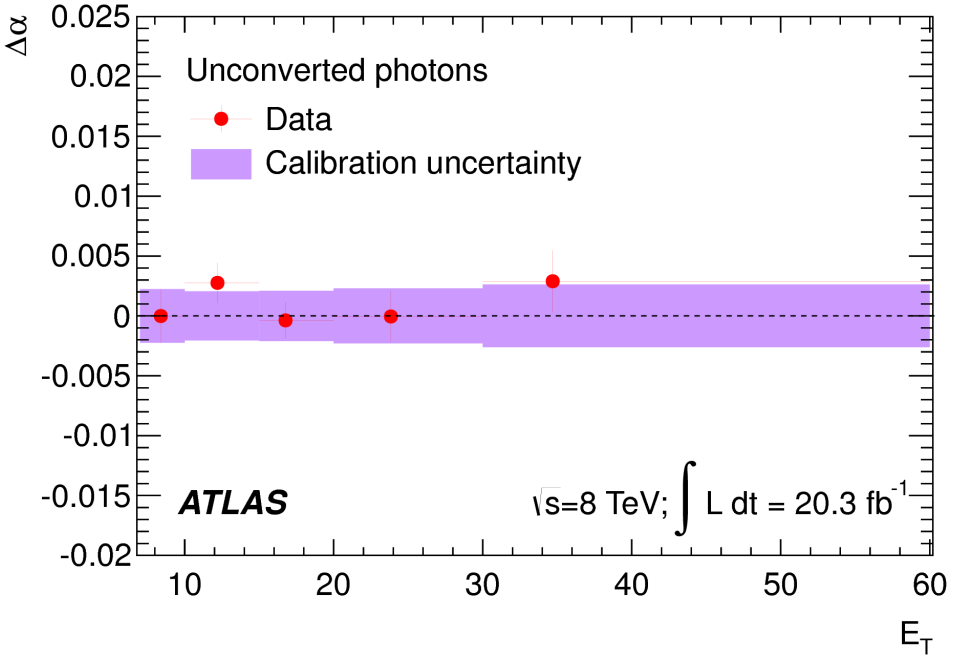

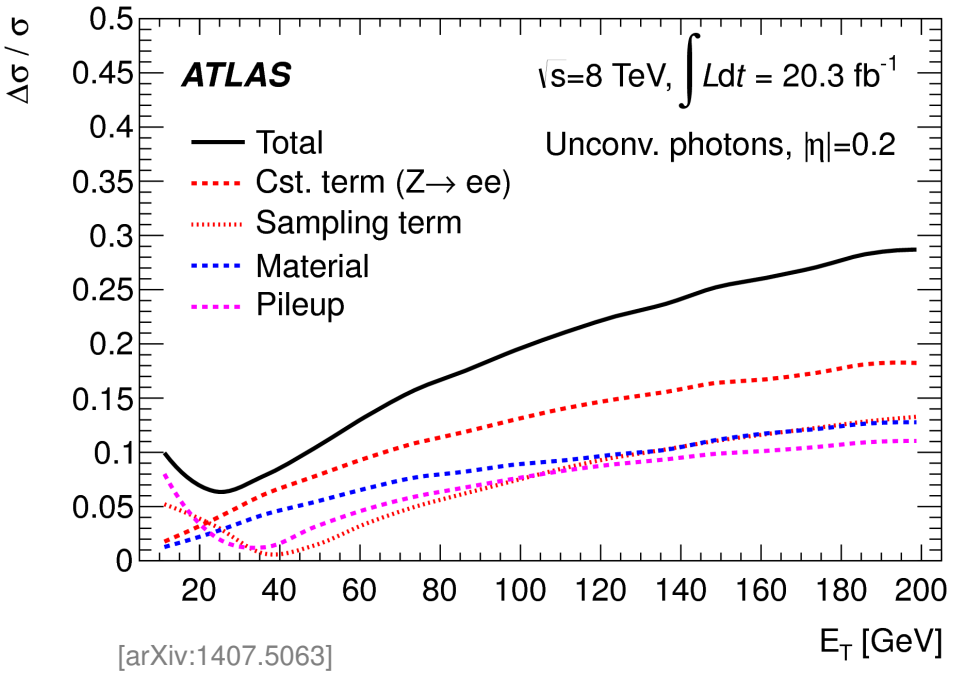

[arXiv:1407.5063]

Photon pointing and primary vertex selection.

$$m_{\gamma\gamma}^2 = 2E_1E_2(1 - \cos\alpha)$$

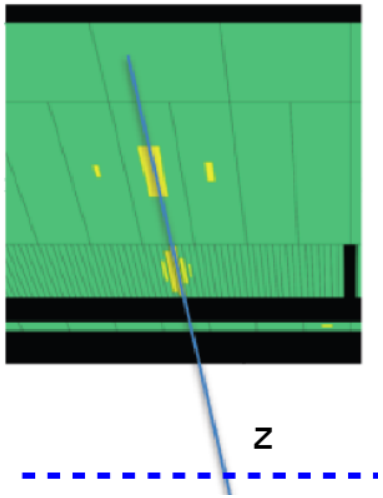

Improve photon angle measurement using

- Photon pointing
  - ⋆ Photon direction from calorimeter using longitudinal segmentation
  - ⋆ Position of conversion vertex for converted photons (with Si hits)
- $\sum p_T^2$, $\sum p_T$ (over tracks) and angular balance in ϕ between tracks and diphoton system (8 TeV)

→ Contribution of angle measurement to mass resolution negligible already without primary vertex information

→ Good primary vertex selection needed for selection of signal jets

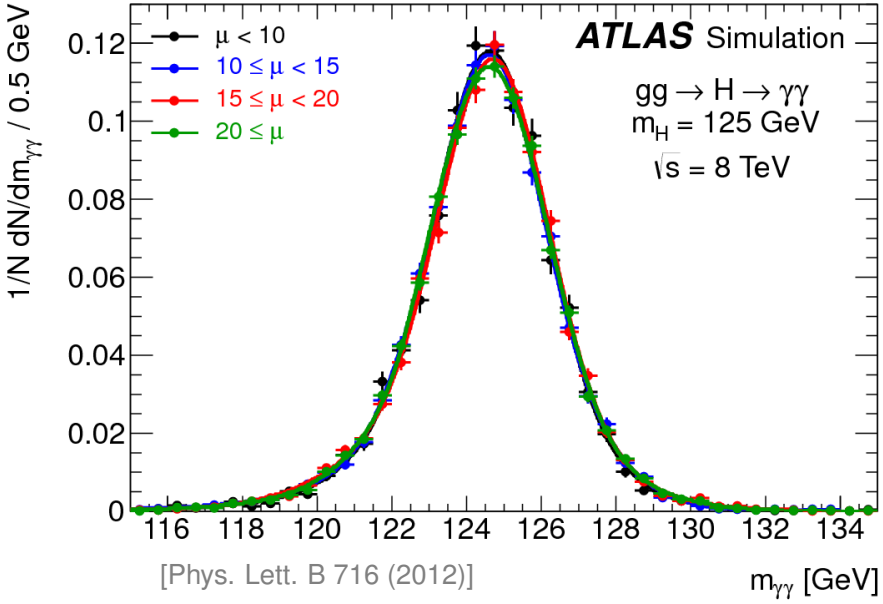

[Phys. Lett. B 716 (2012)]

From discovery to measurements (and searches).

disentangle production modes: couplings to SM particles

differential cross sections

spin

search for $hh \to \gamma\gamma b\bar{b}$

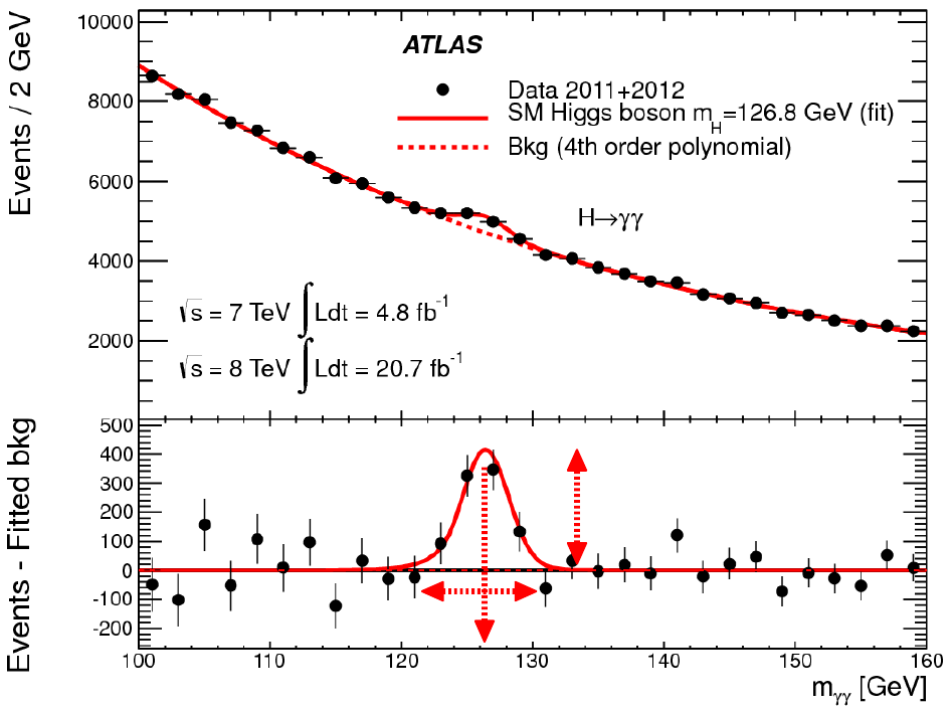

search for FCNC $t \to Hc$

mass measurement

limit on width

search for other narrow resonances with mass of 65-600 GeV

Mass spectrum and background parametrization.

7 TeV + 8 TeV data

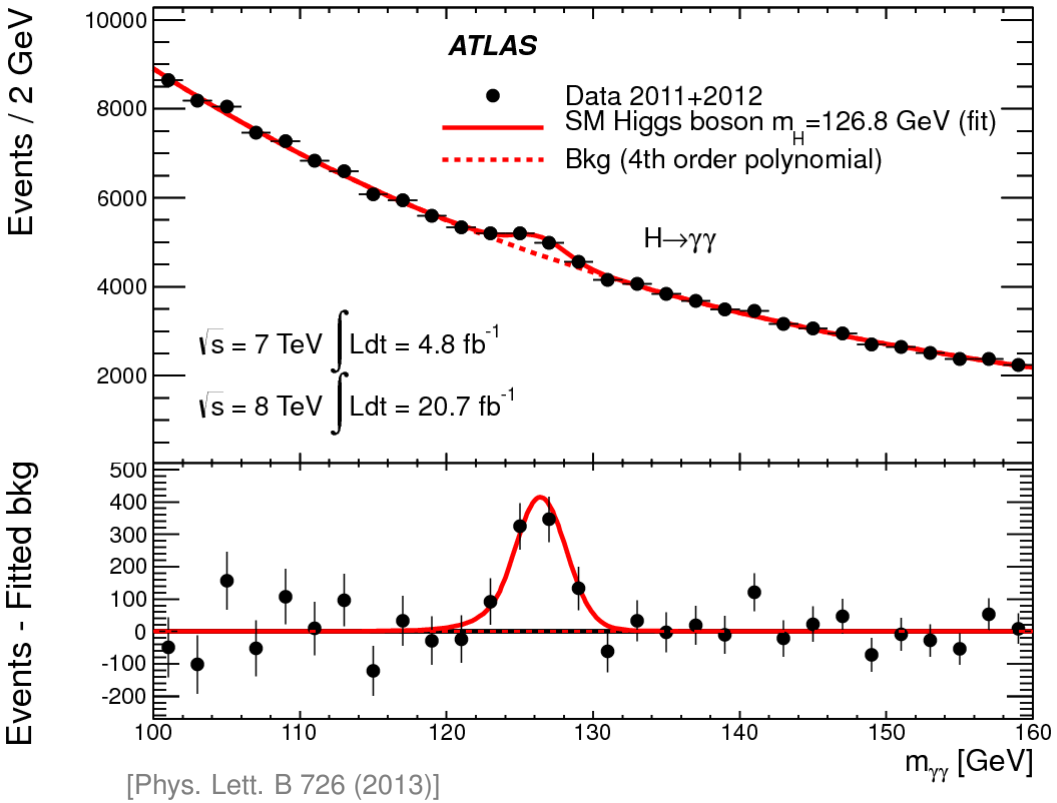

[Phys. Lett. B 726 (2013)]

Background+signal fit, signal fixed at 126.8 GeV

Signal clearly visible ($\sim 6\,\sigma$)

Diphoton selection

Identified and isolated photons
$p_T^{\gamma 1} > 40$ GeV, $p_T^{\gamma 2} > 30$ GeV

23788 events (7 TeV)
118893 events (8 TeV)

Background modelled by 4th order Bernstein polynomial

Studied on high-statistics MC and chosen to give good statistical power while keeping potential biases acceptable

Potential bias accounted for as systematic uncertainty

Mass measurement.

[arXiv:1406.3827]

Dedicated event categorization:
10 categories according to η^{γ}, converted/unconverted γ and p_{Tt}

m_H =125.98±0.42(stat)±0.28(syst) GeV

$\mu = 1.29 \pm 0.30$

- Dominant systematic uncertainty from energy scale

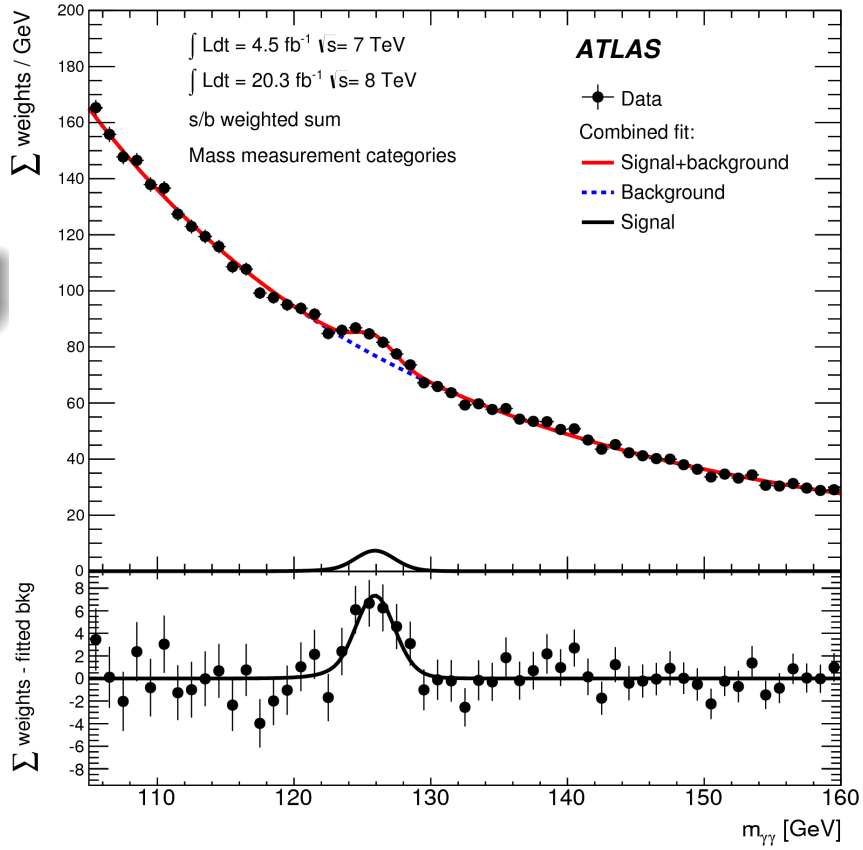

Substantial improvement over previous measurement:

m_H =126.8±0.2±0.7 GeV

- Observed shift consistent with expectation from new calibration (-0.45±0.35 GeV)
- Decreased systematic uncertainty (1/2.5) thanks to improved calibration

Mass measurement: systematic uncertainties.

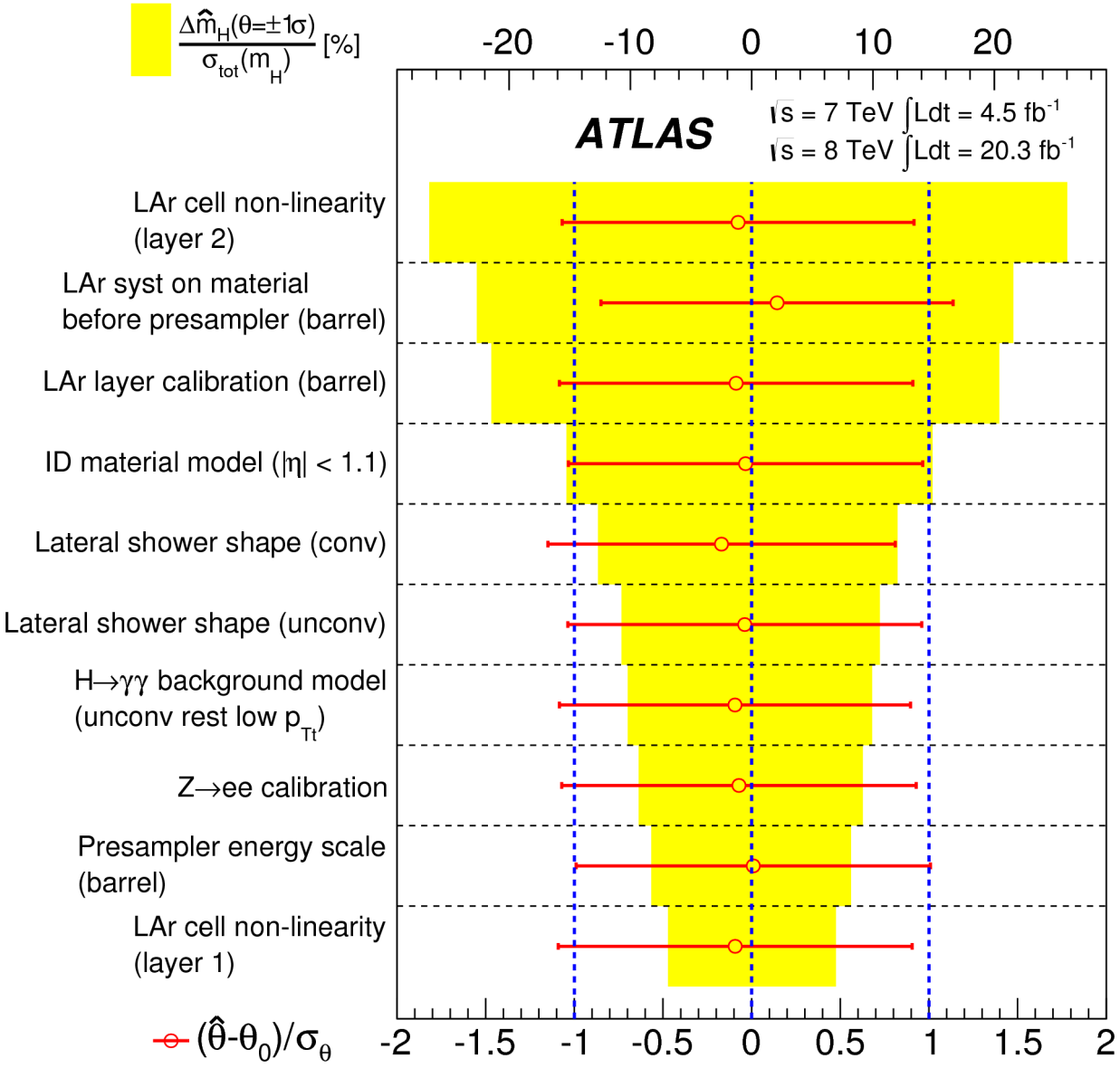

Separating production processes.

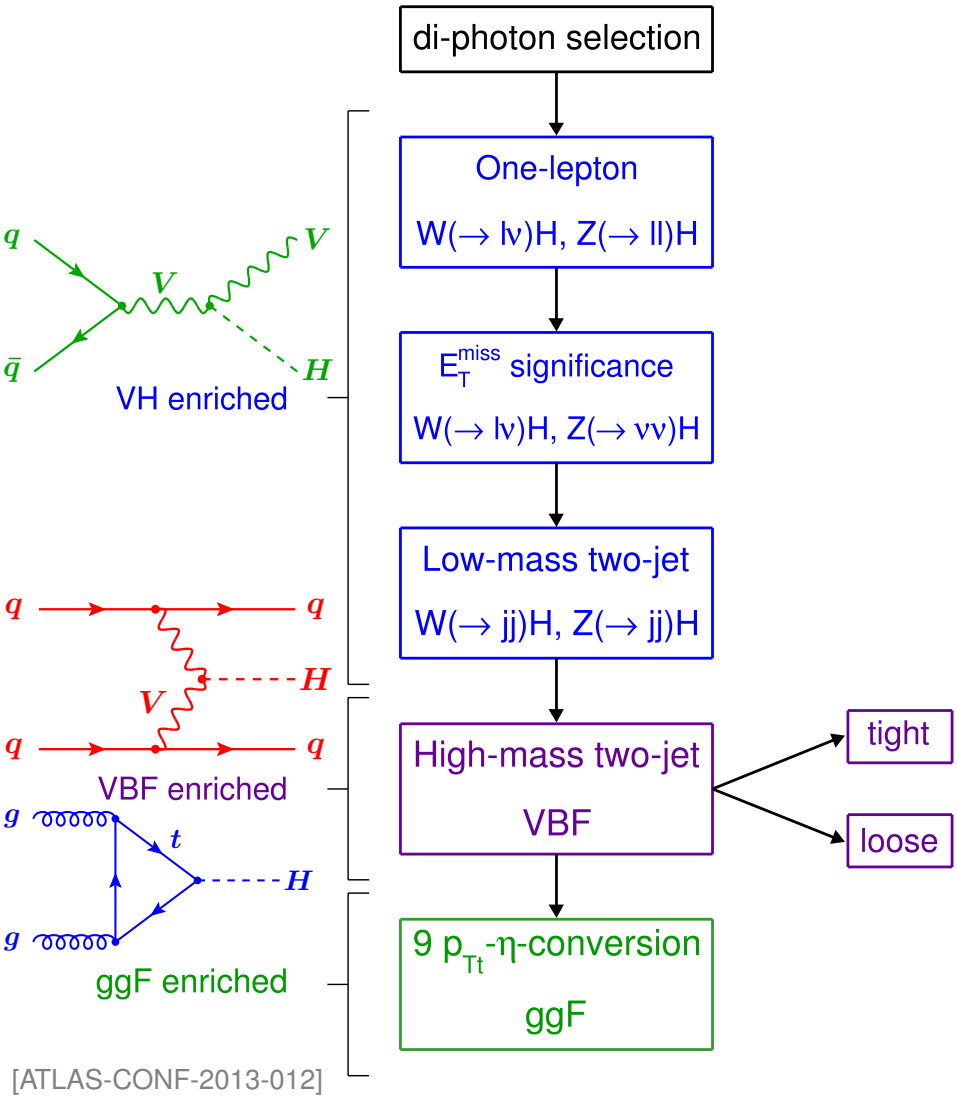

gluon fusion categories according to resolution and S/B

- Dedicated categories for separation of production processes: VH, VBF, gluon fusion
- Remaining events split into categories of varying signal resolution and S/B
  - ★ $\eta_{\gamma 1,2}$, conversions, p_{Tt}

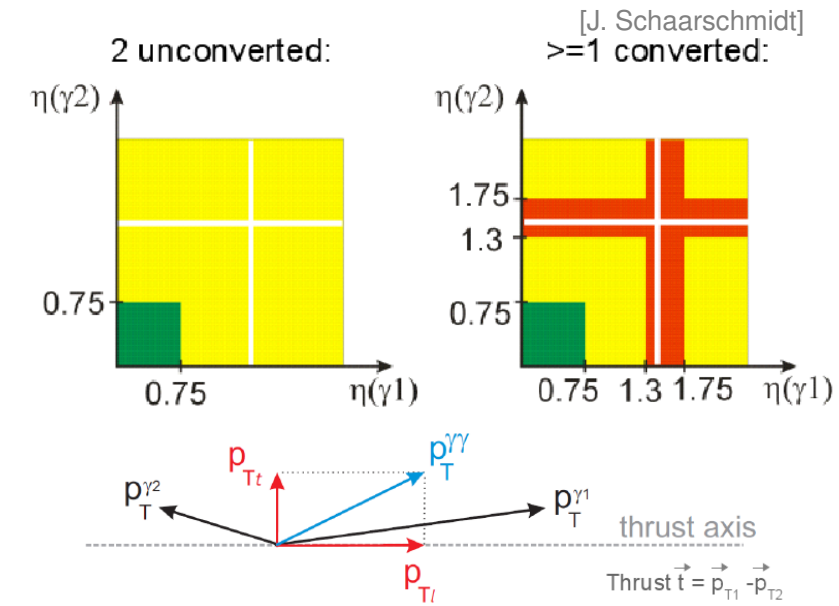

VBF-enriched categories.

Select with 2 jets and VBF topology:

- 2 well-separated jets ($\eta_{j1,2}$, $\Delta\eta_{jj}$, m_{jj})
- Boosted diphoton system ($p_{Tt}^{\gamma\gamma}$)
- Jet-photon separation ($\Delta\phi_{\gamma\gamma;jj}$, $\eta^* = \eta_{\gamma\gamma} - 1/2(\eta_{j1} + \eta_{j2})$, $\Delta R_{\min}^{\gamma j}$)

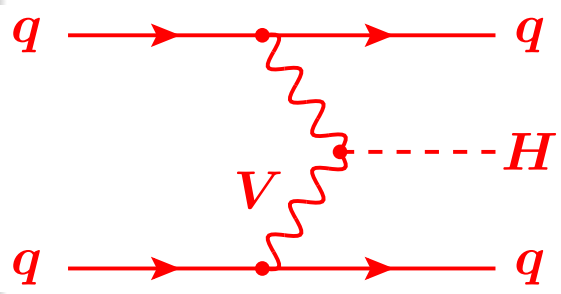

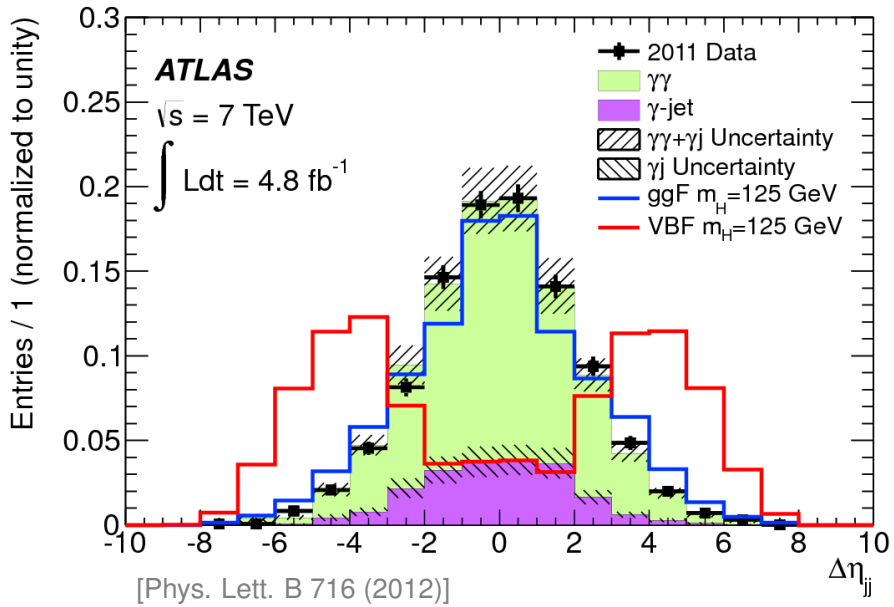

[Phys. Lett. B 716 (2012)]

- Variables combined in a boosted decision tree
- High purity of VBF events

	VBF purity	N_{sig}
tight	76%	8.1
loose	54%	5.3

2-Jets candidate.

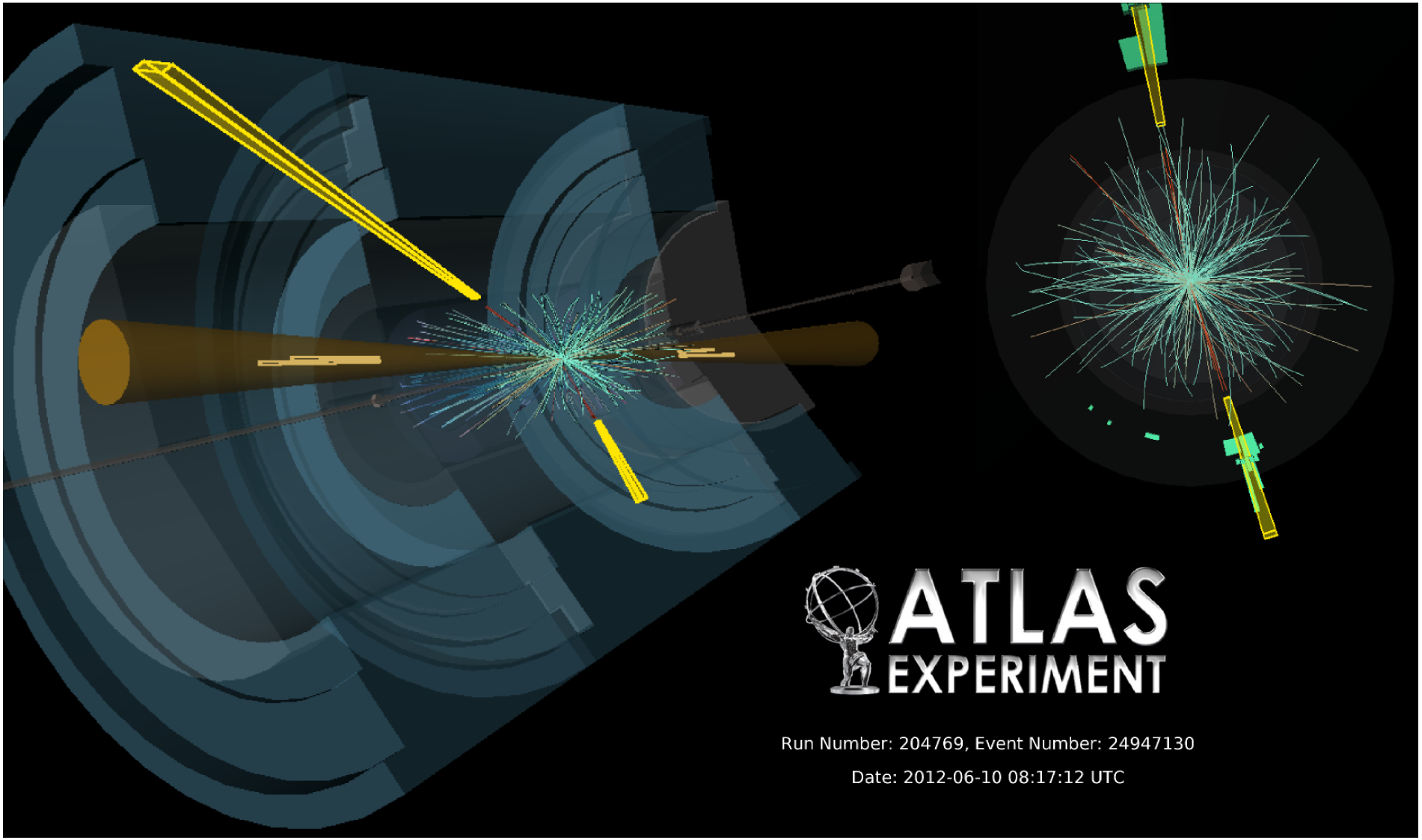

[Phys. Lett. B 726 (2013)]

VH-enriched categories.

Inclusive leptons ($W \to \ell\nu$, $Z \to \ell\ell$)

$p_T^e > 15$ GeV or $p_T^\mu > 10$ GeV, isolated in tracker and calorimeter

Missing transverse momentum ($W \to \ell\nu$, $Z \to \nu\nu$)

E_T^{miss} significance $\frac{E_T^{\text{miss}}}{0.67 \sum E_T} > 5$

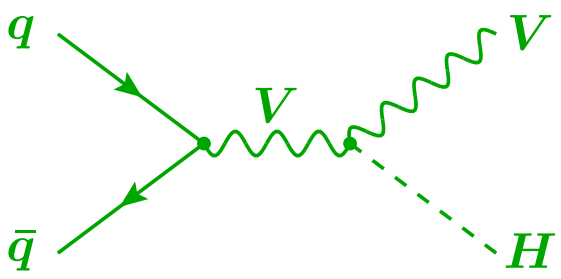

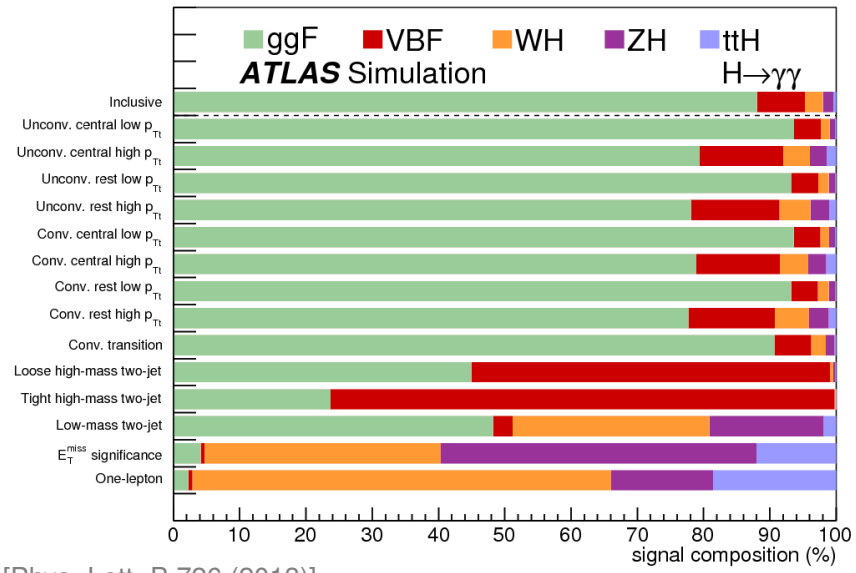

[Phys. Lett. B 726 (2013)]

Dijet ($W \to jj$, $Z \to jj$)

60 GeV $< m_{jj} <$ 110 GeV, $|\Delta\eta_{jj}| < 3.5$

	VH purity	N_{sig}
lepton	82%	2.9
E_T^{miss}	83%	1.3
dijet	47%	3.3

Diphoton mass spectra for a few categories.

Unconverted central, high p_{Tt}

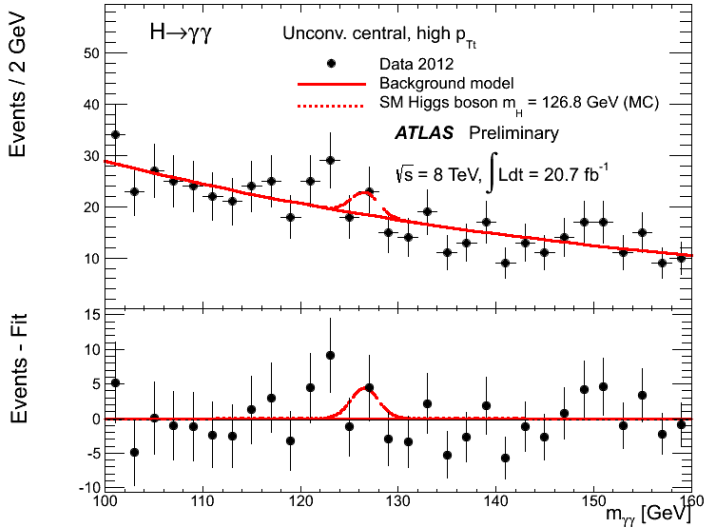

Converted rest, low p_{Tt}

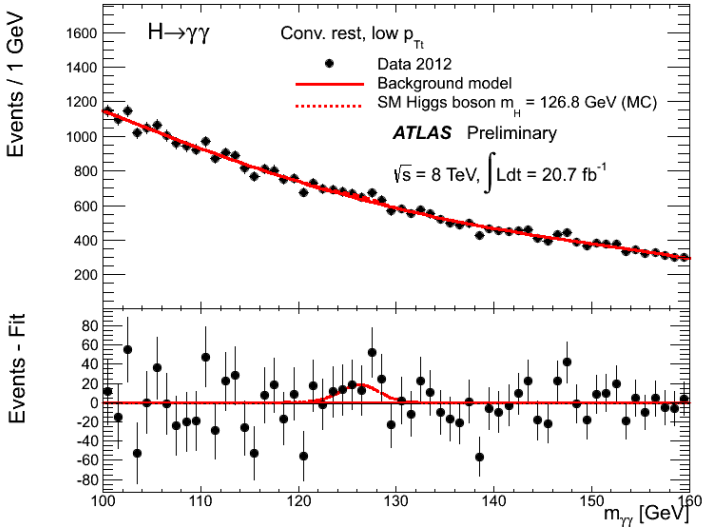

Tight high-mass 2-jet

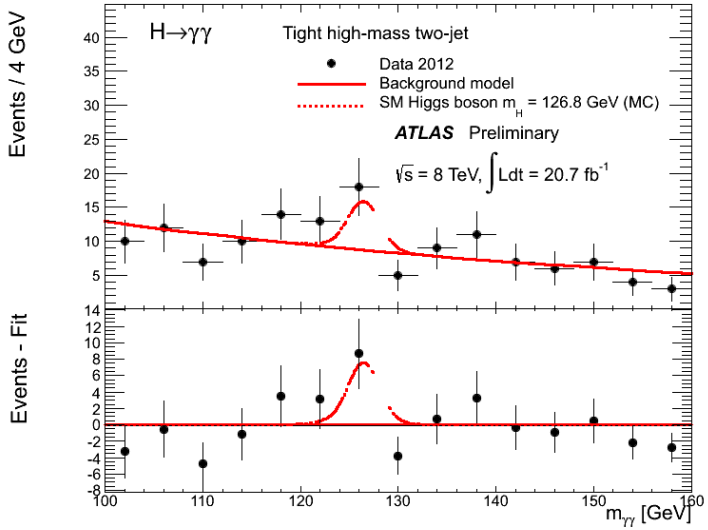

E_T^{miss} significance

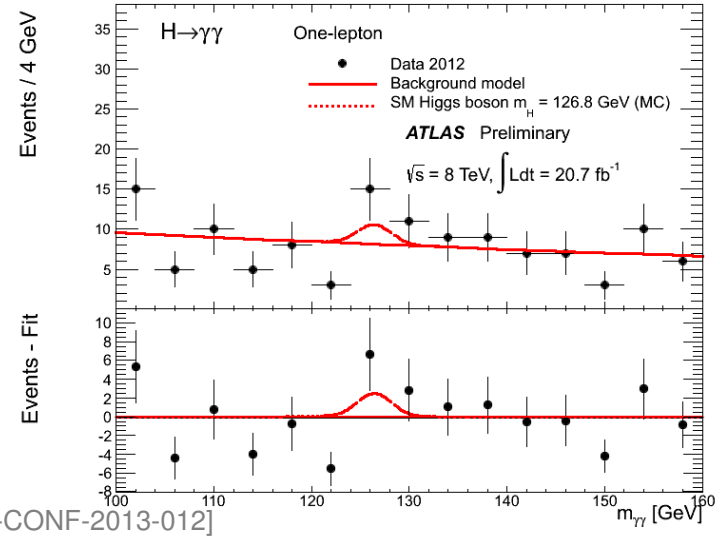

[ATLAS-CONF-2013-012]

Separating production processes.

[Phys. Lett. B 726 (2013)]

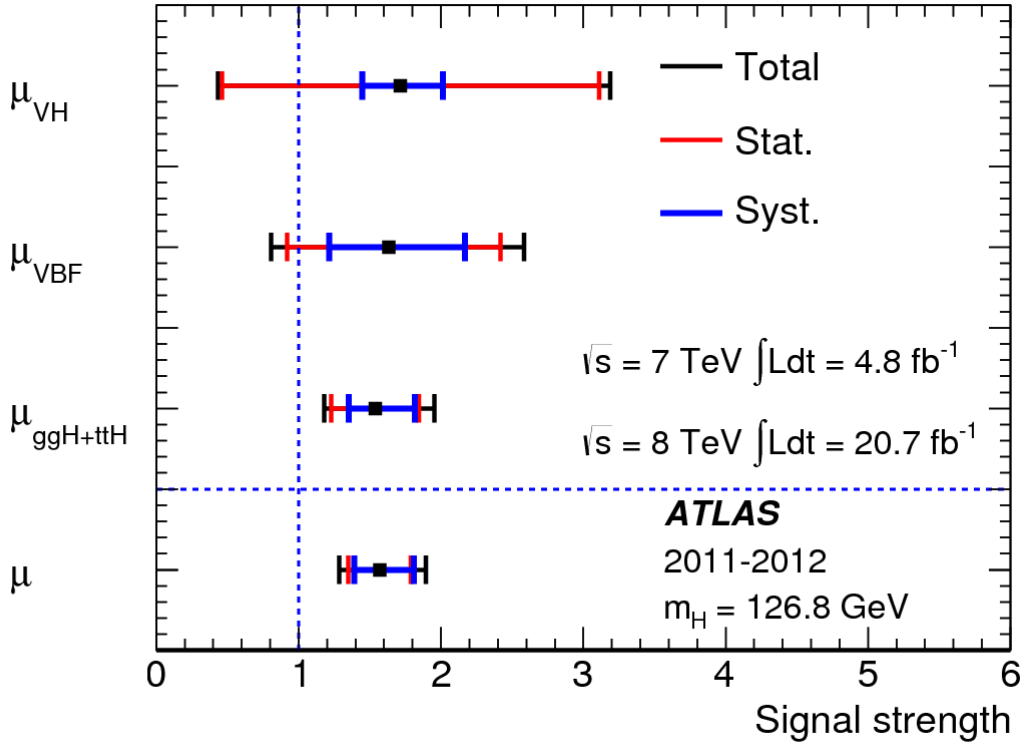

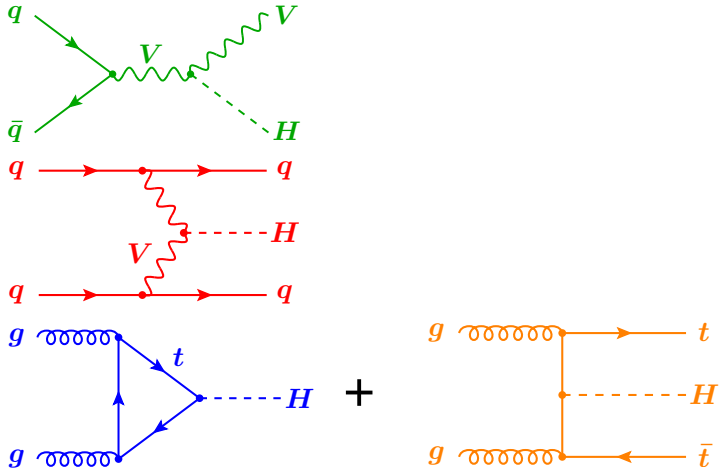

$\mu = 1 \Rightarrow$ SM

μ =1.55±0.23(stat)±0.15(syst)±0.15(theo) (at m_H =125.5 GeV)

Largest contributions to systematic uncertainty

- Invariant mass resolution
- Photon identification efficiency

Have been improved and will be used for the next update

Search for production in association with $t\bar{t}$.

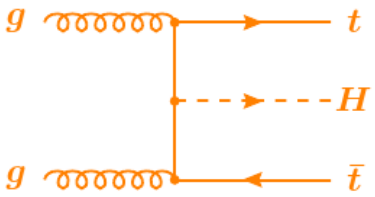

- Aim for high efficiency for $t\bar{t}H$, while suppressing other production modes

Search in two event categories

- Fully hadronic: 2 $t \to bjj'$
  - ★ $\geq$ 6(5) jets ($\geq$ 2(1) b-tagged)
- Leptonic: 1 or 2 $t \to b\ell\nu$
  - ★ $\geq$1 electron or muon
  - ★ $\geq$1 b-tagged jet
  - ★ $E_T^{\text{miss}} > 20$ GeV

- $tHqb$ and WtH production taken into account

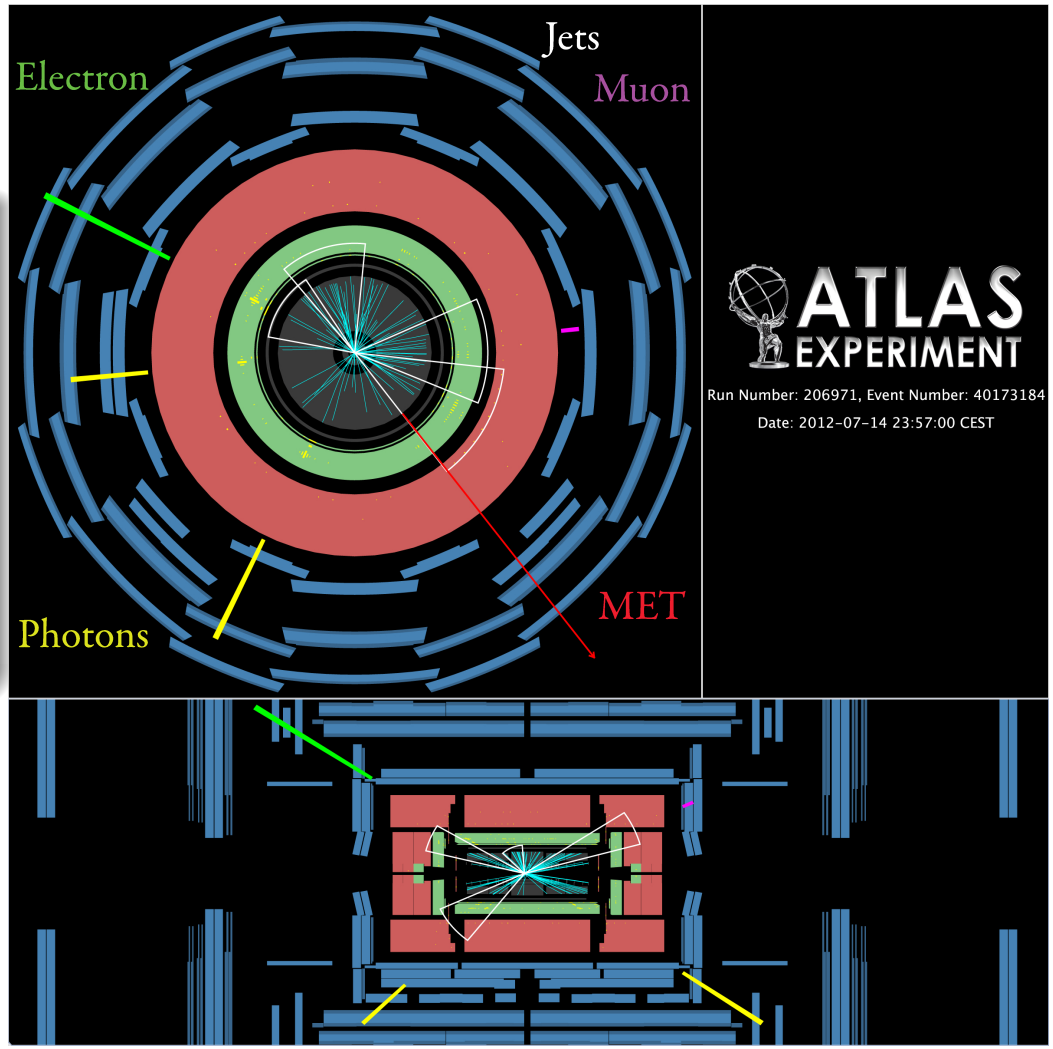

[ATLAS-CONF-2013-080]

Search for production in association with $t\bar{t}$.

Leptonic

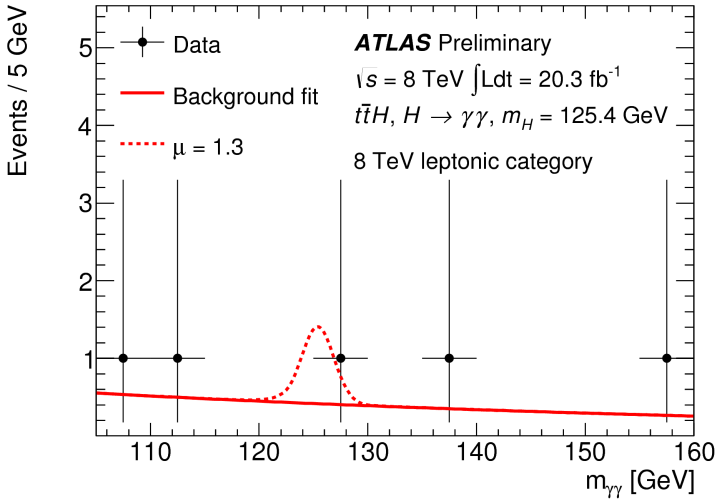

[ATLAS-CONF-2014-043]

0.59	N_H	0.50
0.47	$N_{t\bar{t}H}$	0.42
80%	Purity	84%

(8 TeV)

Hadronic

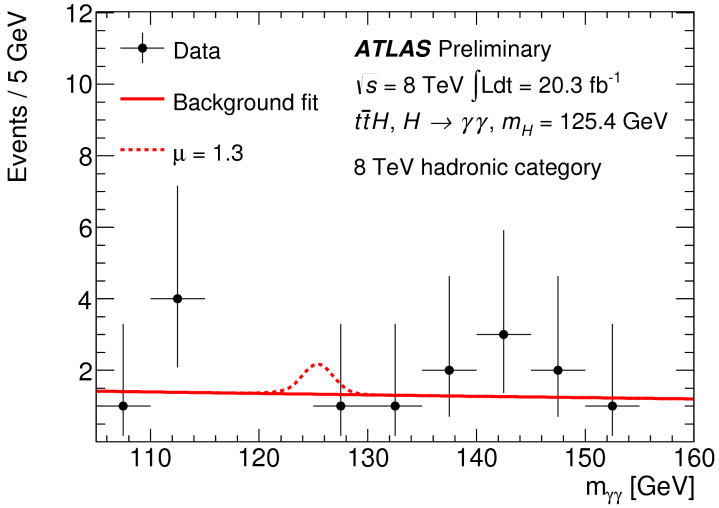

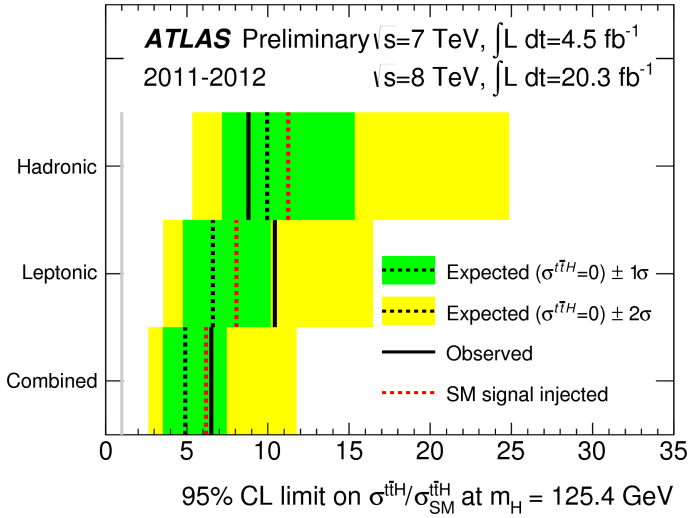

- Assume SM for other production modes and BR($H \to \gamma\gamma$)

$\sigma^{t\bar{t}H}/\sigma^{t\bar{t}H}_{\mathrm{SM}} < 6.5$ @ 95% CL

(4.9 expected) at m_H=125.4 GeV

Detailed coupling studies: combination with the other decay channels

Combining with the other decay channels.

$H \to ZZ^*$
$\to 4\ell$

[Phys. Lett. B 726 (2013)]

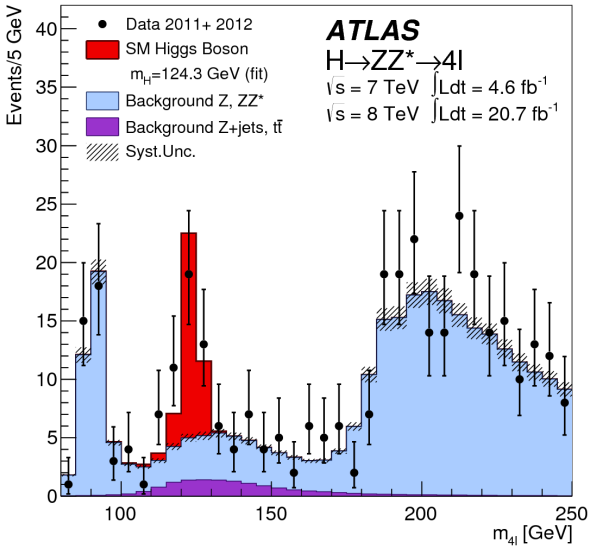

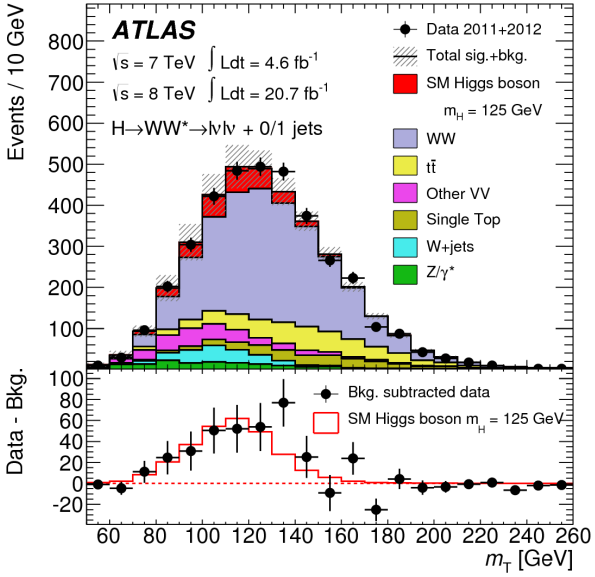

$H \to WW^*$
$\to 2\ell 2\nu$

[Phys. Lett. B 726 (2013)]

$H \to \tau\tau$

[ATLAS-CONF-2013-108]

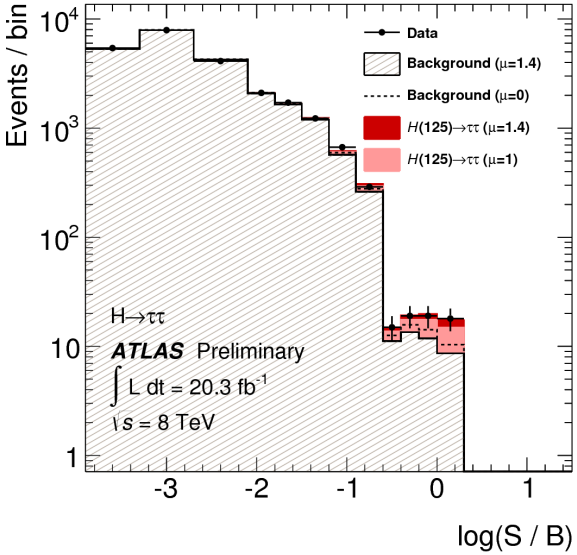

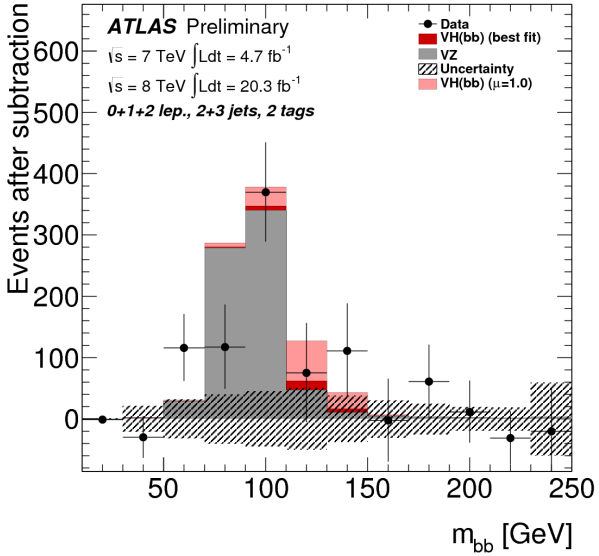

$H \to b\bar{b}$

[ATLAS-CONF-2013-079]

Separating production channels.

- Coupling to vector bosons
  use $\mu_{\mathrm{VBF+VH}} = \mu_{\mathrm{VBF}} = \mu_{\mathrm{VH}}$
- Coupling to fermions
  use $\mu_{\mathrm{ggF+ttH}} = \mu_{\mathrm{ggF}} = \mu_{\mathrm{ttH}}$

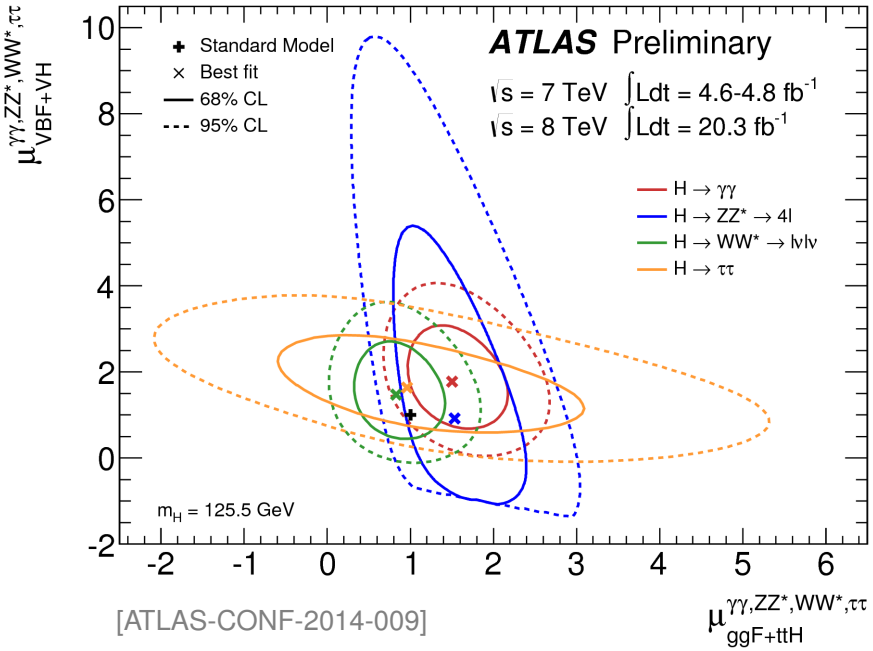

[ATLAS-CONF-2014-009]

- Combination of decay channels (at level of μ) would need assumptions on BRs

[ATLAS-CONF-2014-009]

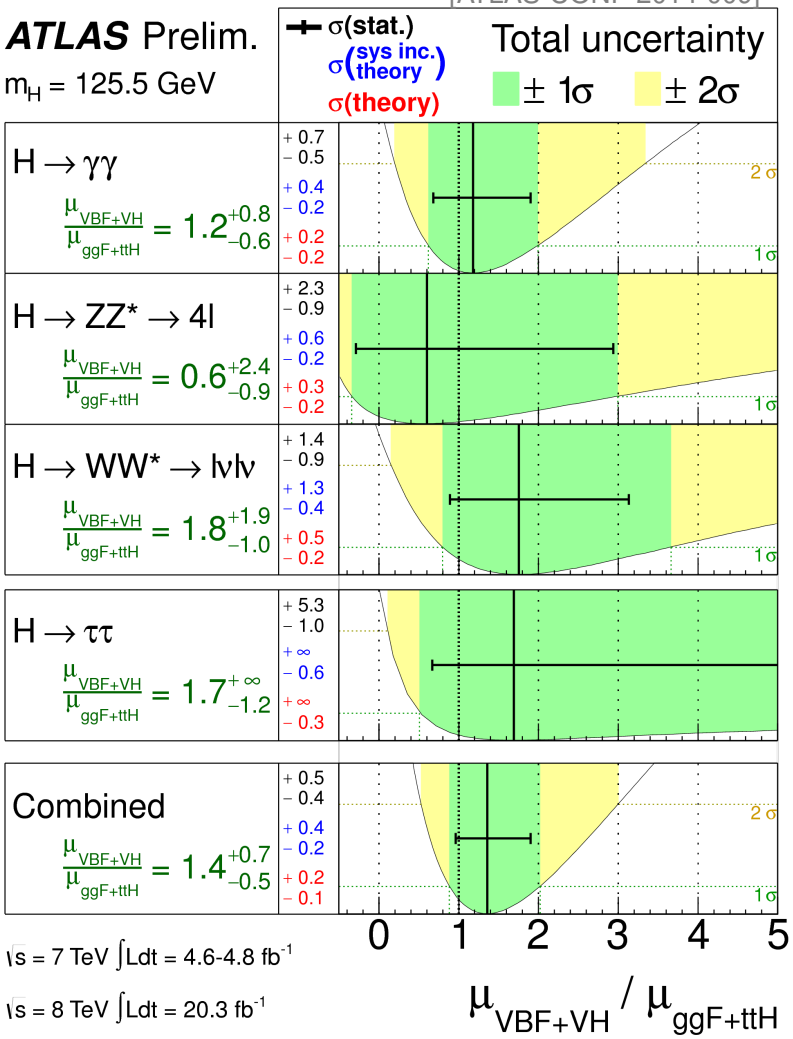

$4.1\,\sigma$ evidence for VBF

(obtained profiling μ_{VH})

Detailed coupling studies.

- LO-inspired coupling scale factors κ_j:

$$\mathcal{L} = \kappa_3 \frac{m_H^2}{2v} H^3 + \kappa_Z \frac{m_Z^2}{v} Z_\mu Z^\mu H + \kappa_W \frac{2m_W^2}{v} W_\mu^+ W^{-\mu} H$$
$$+ \kappa_g \frac{\alpha_s}{12\pi v} G^a_{\mu\nu} G^{a\mu\nu} H + \kappa_\gamma \frac{\alpha}{2\pi v} A_{\mu\nu} A^{\mu\nu} H + \kappa_{Z\gamma} \frac{\alpha}{\pi v} A_{\mu\nu} Z^{\mu\nu} H$$
$$+ \kappa_{VV} \frac{\alpha}{2\pi v} \left(\cos^2\theta_W Z_{\mu\nu} Z^{\mu\nu} + 2\, W^+_{\mu\nu} W^{-\mu\nu}\right) H$$
$$- \left(\kappa_t \sum_{f=u,c,t} \frac{m_f}{v} f\bar{f} + \kappa_b \sum_{f=d,s,b} \frac{m_f}{v} f\bar{f} + \kappa_\tau \sum_{f=e,\mu,\tau} \frac{m_f}{v} f\bar{f} \right) H.$$

- κ_j defined such that $\kappa_j = 1$ for SM (including higher-order corrections)
- Effective coupling scale factors κ_γ and κ_g treated as function of more fundamental scale factors κ_t, κ_b, κ_W, ... for some tests

Specific benchmark models.

Probing fermion and boson couplings

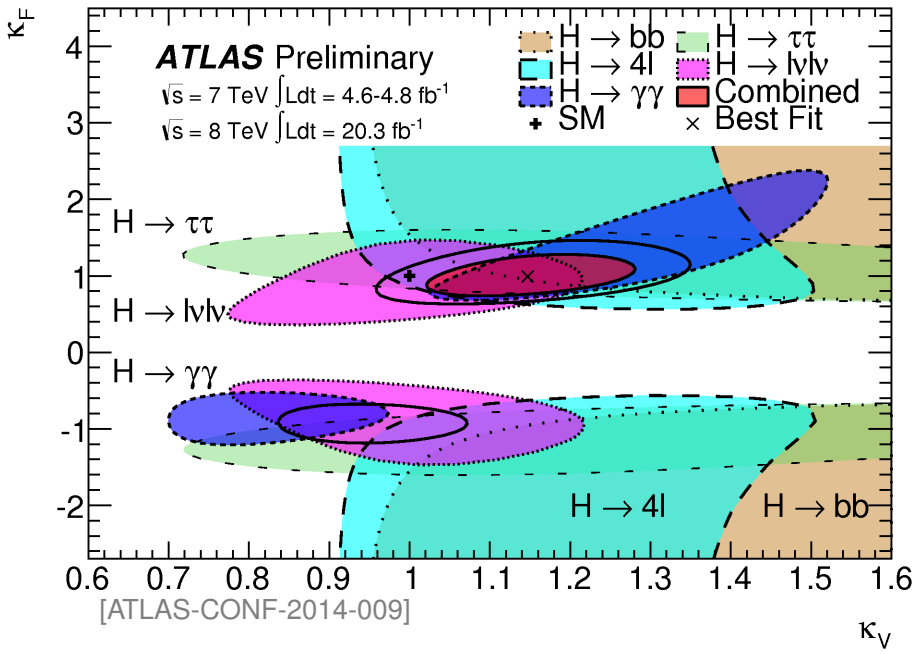

- Simplest non-trivial model
- $H \to \gamma\gamma$ decay gives sensitivity to relative sign
- Agreement of SM hypothesis with data ∼10%

Probing custodial symmetry

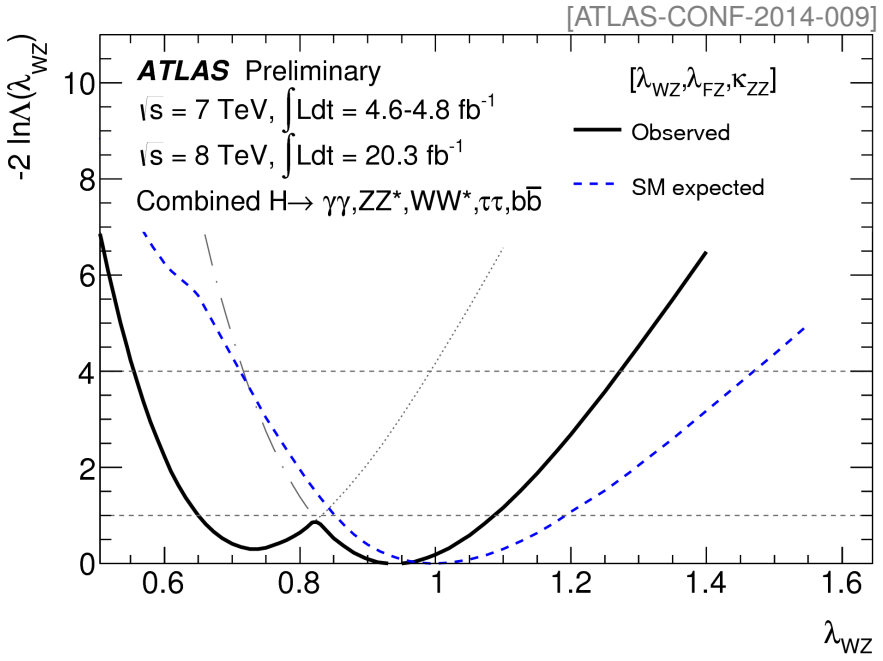

- $\lambda_{WZ} = \kappa_W / \kappa_Z$
  - ⋆ Common κ_F for fermion couplings
- Agreement of SM hypothesis with data ∼19%

Probing beyond SM contributions.

Effective scale factors κ_g and κ_γ allow for new contributions in loops

[ATLAS-CONF-2014-009]

Only SM contributions to total width

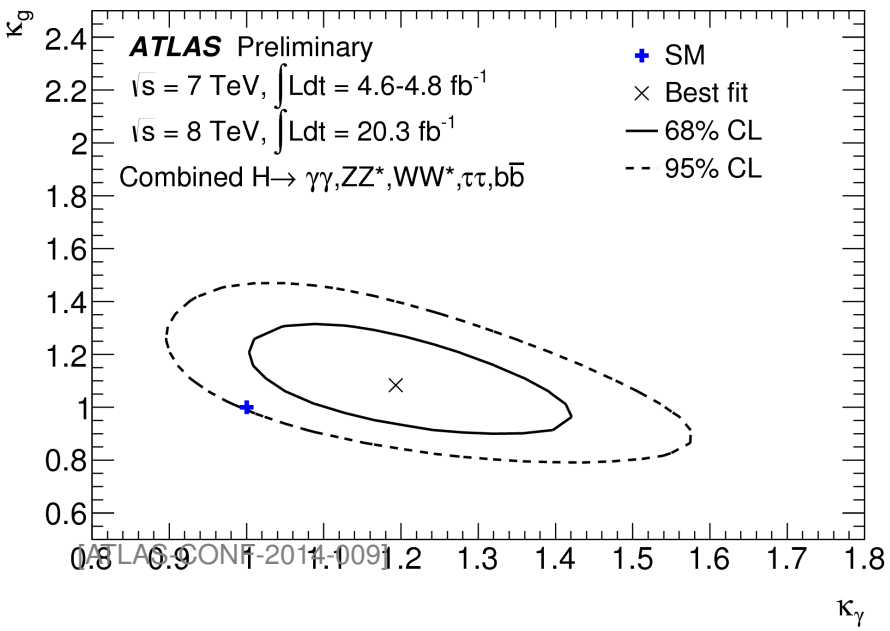

[ATLAS-CONF-2014-009]

- Agreement of SM hypothesis with data ∼9%

No assumptions on total width

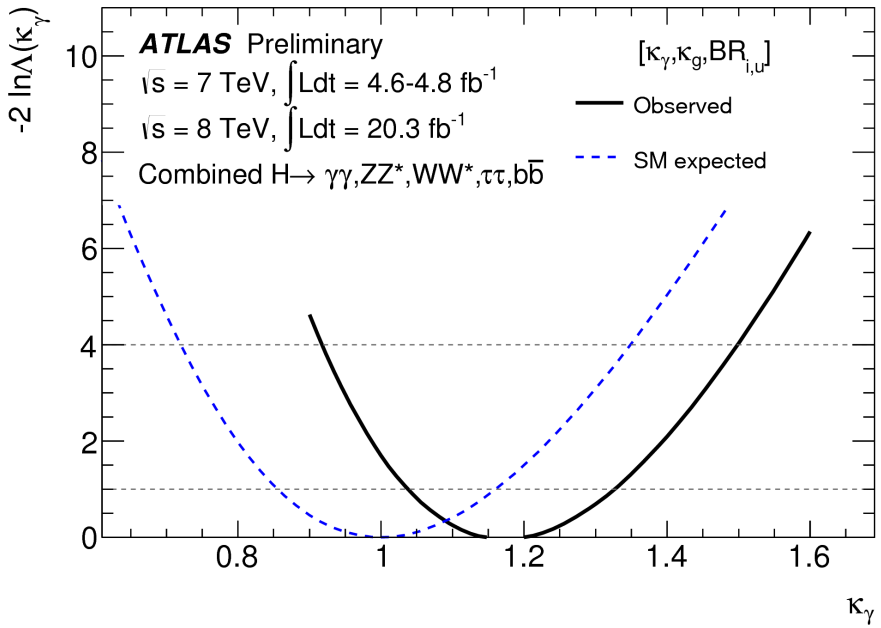

- Allow for undetected or invisible final states
- $\mathrm{BR}_{i,u} < 0.41$ (at 95% CL) (expected: 0.55)

Most generic model.

...free couplings to SM particles and allowing for deviations in loops and additional contributions to total width

- No sensitivity to relative signs between couplings
- No sensitivity to Higgs-top coupling
  - ⋆ Degenerate with gluon-fusion loop
  - ⋆ Needs observation of ttH production
- Agreement of SM hypothesis with data ∼21%

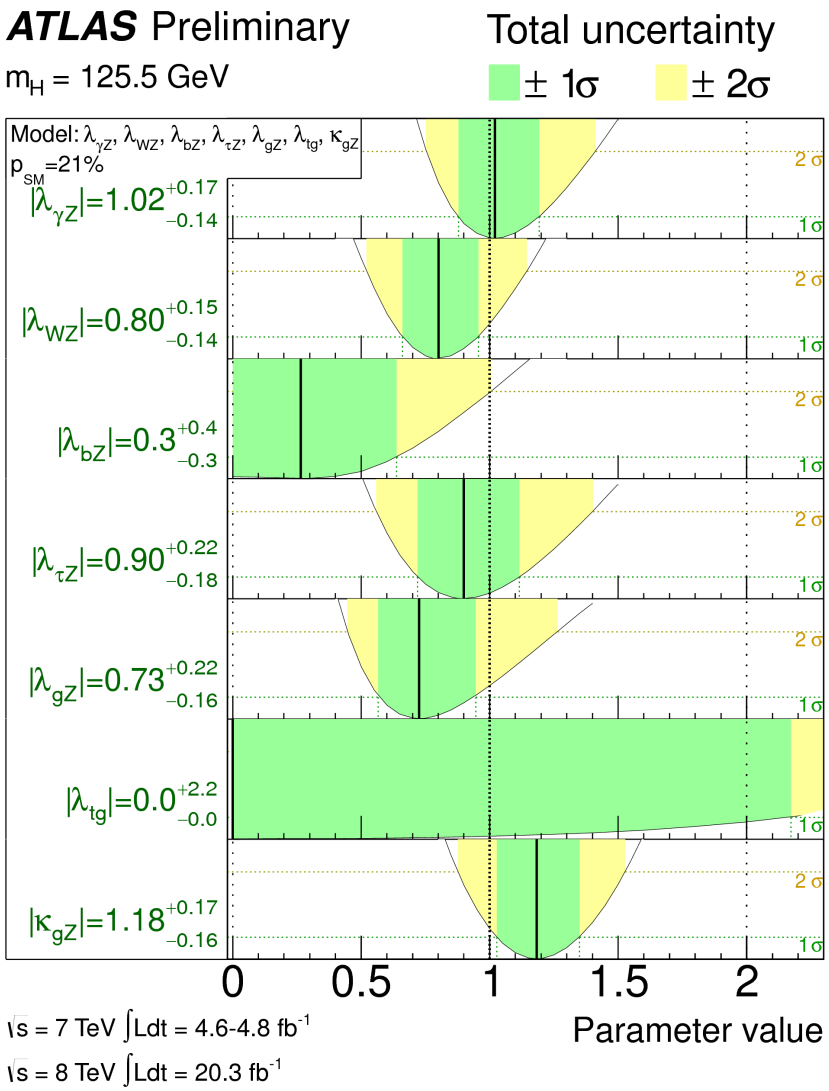

[ATLAS-CONF-2014-009]

Back to $H \to \gamma\gamma$

Differential cross section measurements.

Full 8 TeV dataset allows to make first differential cross section measurements

- Almost model-independent measurements of production and decay kinematics
- Measure kinematic distributions of Higgs, of associated jets, ...

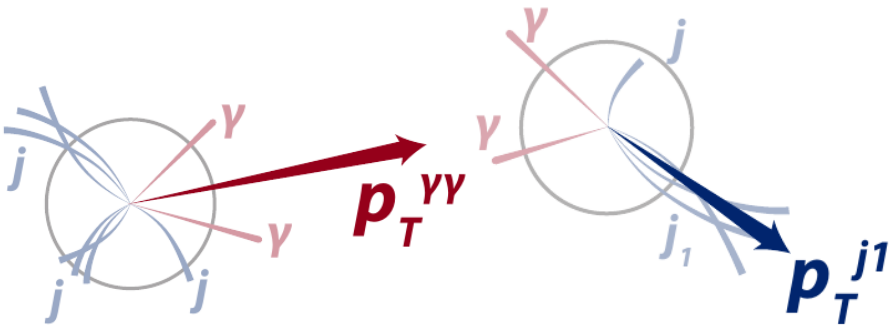

- $H \to \gamma\gamma$ decay well suited thanks to good resolution and "high" signal yield
- Background subtracted in a simultaneous signal-plus-background fit to all bins

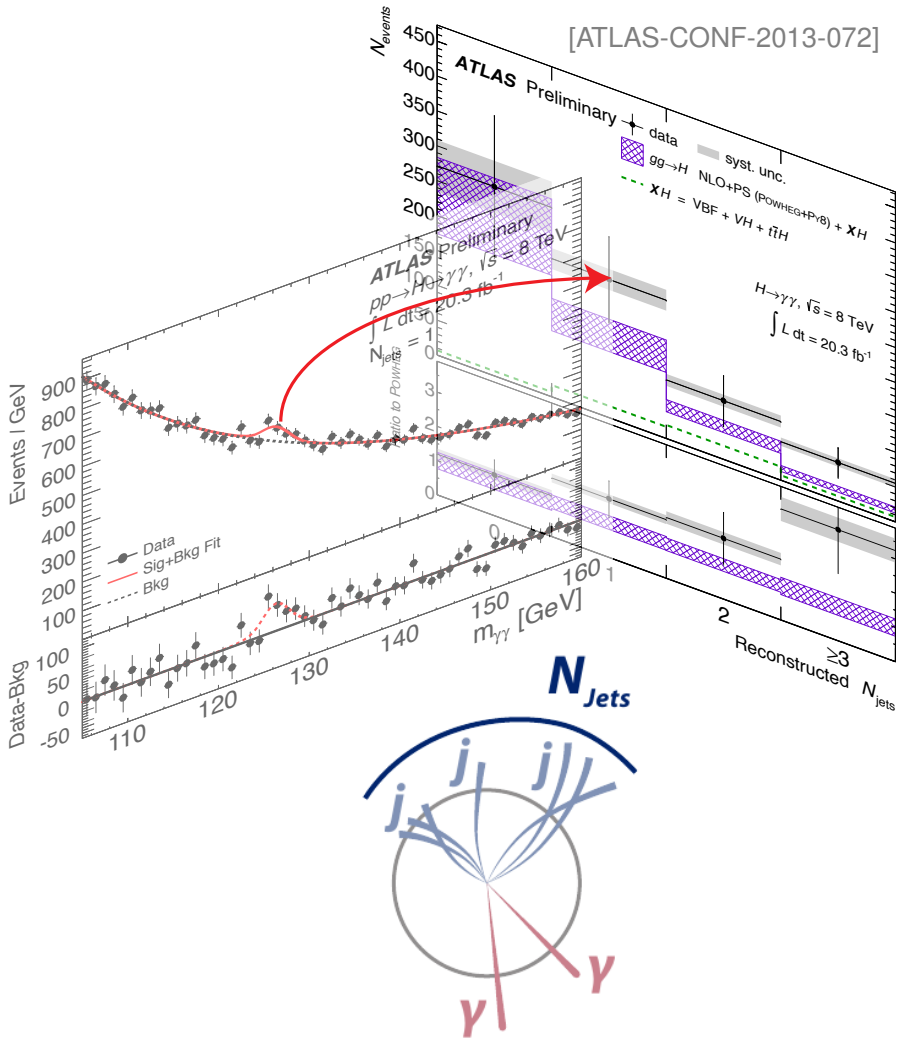

Differential cross section measurements.

- Bin-by-bin unfolding for detector acceptance, resolution and efficiency
- Unfold to fiducial region defined by photons (and jets)
  - ⋆ $p_T^{\gamma 1(\gamma 2)} > 0.35\ (0.25)\ m_{\gamma\gamma}, \quad |\eta^{\gamma 1,2}| < 2.37$
  - ⋆ $p_T^j > 30$ GeV, $\quad |y^j| < 4.4$

[arXiv:1407.4222]

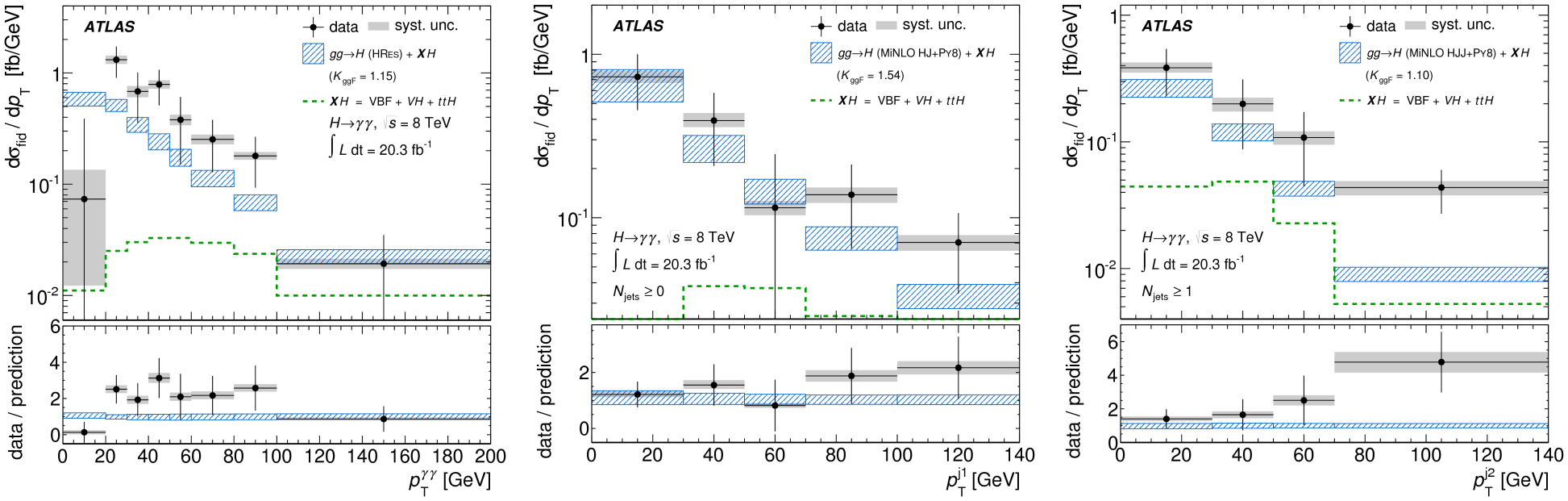

- Differential measurements presently dominated by statistical uncertainties
- Data and predictions agree within current uncertainties

Fiducial cross section measurements.

Fiducial cross sections with specific signatures and topologies

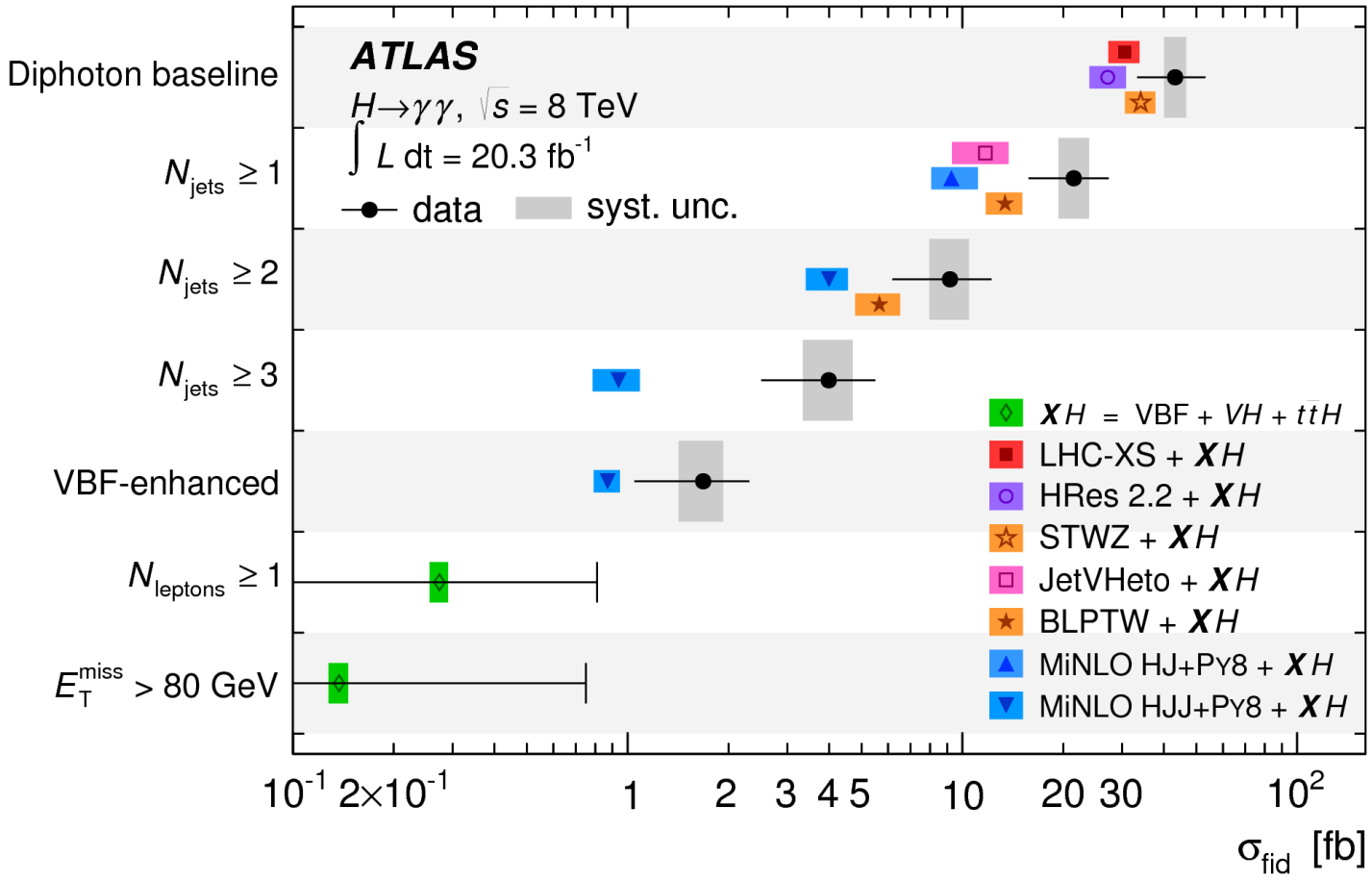

Theory predictions with LBL contributions

- Agreement with predictions to $1 - 2\,\sigma$

$$\sigma_{\rm fid}(pp \to H \to \gamma\gamma) = 43.2 \pm 9.4({\rm stat})^{+3.2}_{-2.9}({\rm syst}) \pm 1.2({\rm lumi})\ {\rm fb}$$

Conclusions and outlook.

- Successful transition from Higgs search to Higgs measurements over the past two years
- Precise measurement of mass, measurements of couplings, differential cross sections, limits on width, ...
- Most measurements currently limited by statistical uncertainties
  - ⋆ Effort to improve calibration, efficiency measurements, ... paid off

→ Precision of measurements will improve with larger datasets in Run2

- But will also have to work hard to improve systematic uncertainties

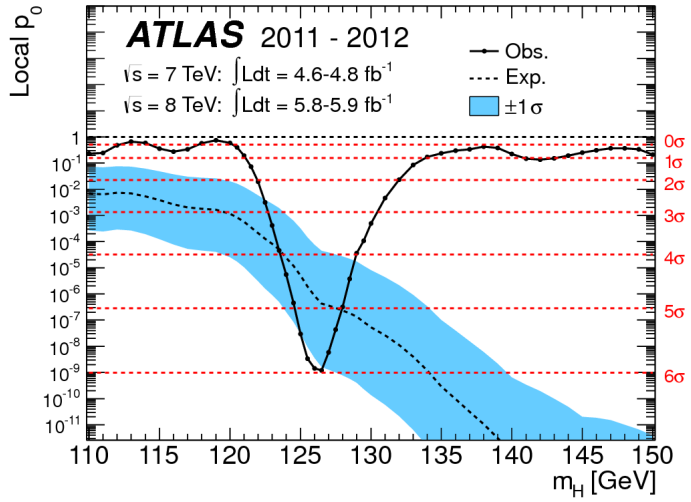

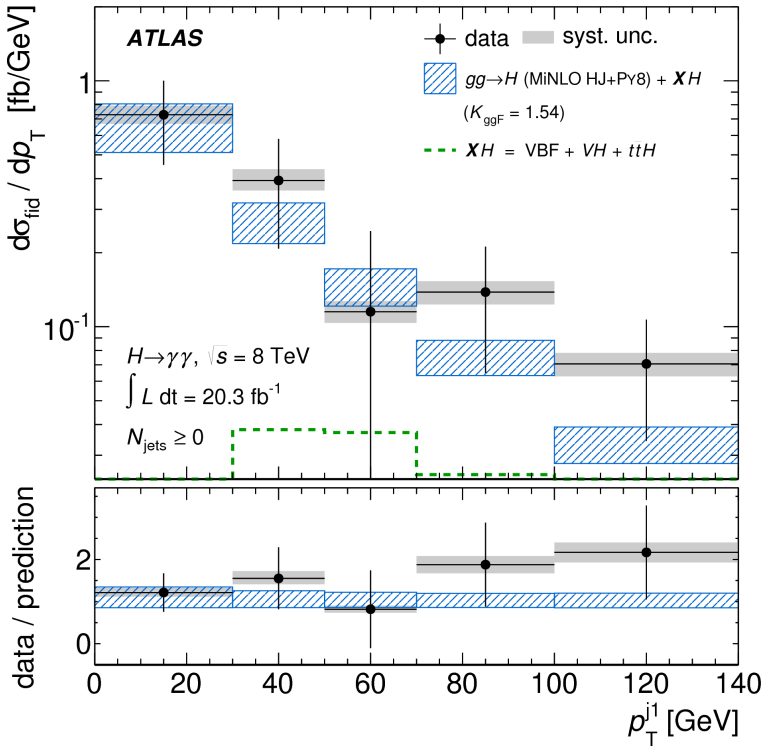

Mass measurement: statistical uncertainties.

m_H = 125.98 ± 0.42 (stat) ± 0.28 (syst) GeV (μ = 1.29 ± 0.30)

to be compared with:

The previous measurement: 126.8 ± 0.2 ± 0.7 GeV

- observed shift (0.8 GeV) consistent with expected shift -0.45 ± 0.35 GeV
- syst. error decreased by factor 2.5
- stat. error:

	μ	Exp. σ	Obs. σ
Previous	1.55	0.33 GeV	0.24 GeV
Current	1.29	0.35 GeV	0.42 GeV

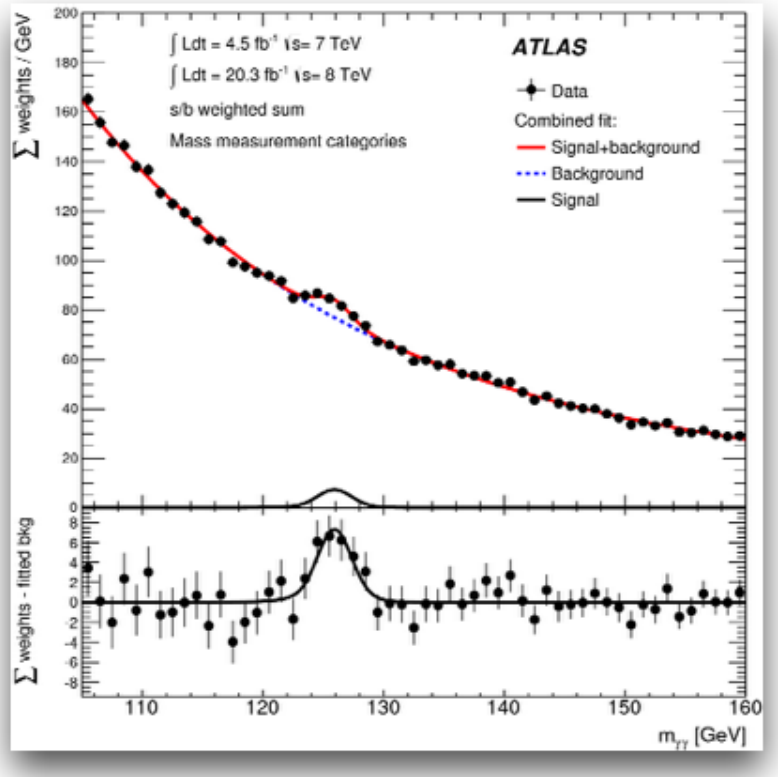

(S. Laplace)